AD-A131 272 THEORY OF VISCOPLASTIC SHELLS FOR DYNAMIC RESPONSE(U) 1/1
WEIDLINGER ASSOCIATES NEW YORK R S ATKATSH ET AL.
01 JAN 82 DNA-TR-81-50 DNA001-81-C-0048

UNCLASSIFIED F/G 13/13 NL

END
FILMED
DTIC

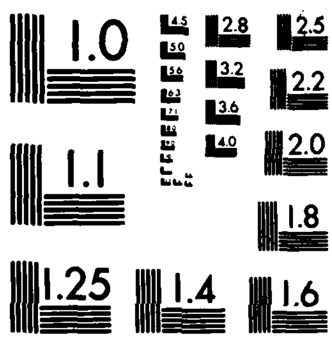
1.0
2.8
2.5
3.2
2.2
3.6
4.0
2.0
1.1
1.8
1.25
1.4
1.6

(12)

DNA-TR-81-50

THEORY OF VISCOPLASTIC SHELLS FOR DYNAMIC RESPONSE

Weidlinger Associates, Consulting Engrg
333 Seventh Ave
New York, New York 10001

1 January 1982

echnical Report

ADA131272

CONTRACT No. DNA 001-81-C-0048

APPROVED FOR PUBLIC RELEASE;
DISTRIBUTION UNLIMITED.

THIS WORK WAS SPONSORED BY THE DEFENSE NUCLEAR AGENCY
UNDER RDT&E RMSS CODE B344081466 Y99QAXSF00002 H2590D.

Prepared for
Director
DEFENSE NUCLEAR AGENCY
Washington, DC 20305

UNCLASSIFIED

SECURITY CLASSIFICATION OF THIS PAGE (When Data Entered)

REPORT DOCUMENTATION PAGE		READ INSTRUCTIONS BEFORE COMPLETING FORM
1. REPORT NUMBER DNA-TR-81-50	2. GOVT ACCESSION NO. A131 242	3. RECIPIENT'S CATALOG NUMBER
4. TITLE (and Subtitle) THEORY OF VISCOPLASTIC SHELLS FOR DYNAMIC RESPONSE		5. TYPE OF REPORT & PERIOD COVERED Technical Report 6. PERFORMING ORG. REPORT NUMBER
7. AUTHOR(s) R. S. Atkatsh M. P. Bieniek I. S. Sandler		8. CONTRACT OR GRANT NUMBER(s) DNA 001-81-C-0048
9. PERFORMING ORGANIZATION NAME AND ADDRESS Weidlinger Associates, Consulting Engrg 333 Seventh Avenue New York, New York 10001		10. PROGRAM ELEMENT, PROJECT, TASK AREA & WORK UNIT NUMBERS Task Y99QAXSF-00002
11. CONTROLLING OFFICE NAME AND ADDRESS Director Defense Nuclear Agency Washington, DC 20305		12. REPORT DATE 1 January 1982 13. NUMBER OF PAGES 68
14. MONITORING AGENCY NAME & ADDRESS(if different from Controlling Office)		15. SECURITY CLASS (of this report) UNCLASSIFIED 15a. DECLASSIFICATION/DOWNGRADING SCHEDULE N/A

16. DISTRIBUTION STATEMENT (of this Report)

Approved for public release; distribution unlimited.

17. DISTRIBUTION STATEMENT (of the abstract entered in Block 20, if different from Report)

18. SUPPLEMENTARY NOTES

This work was sponsored by the Defense Nuclear Agency under RDT&E RMSS Code B344081466 Y99QAXSF00002 H2590D.

19. KEY WORDS (Continue on reverse side if necessary and identify by block number)

Viscoplasticity
Dynamic Response
Shell Analysis
EPSA Finite Element Code
Strain Rate Effects

20. ABSTRACT (Continue on reverse side if necessary and identify by block number)

Viscoplastic shell model is formulated which utilizes the shell membrane strains and curvatures as the kinematic variable and the shell stress resultants as the dynamic variables.

The viscoplastic shell model combines the concept of Perzyna's viscoplastic constitutive equations with Bieniek's shell stress resultant formulation. The model is incorporated into the EPSA code for the analysis of shells in an

DD FORM 1 JAN 73 1473 EDITION OF 1 NOV 65 IS OBSOLETE

UNCLASSIFIED

SECURITY CLASSIFICATION OF THIS PAGE (When Data Entered)

20. ABSTRACT (Continued)

acoustic medium subjected to dynamic loading which produce large elasto-viscoplastic deformations in the shell. Several examples are presented to exhibit the effect of material rate dependence upon structural response.

Conversion factors for U.S. customary to metric (SI) units of measurement

To Convert From	To	Multiply By
angstrom	meters (m)	1.000 000 X E -10
atmosphere (normal)	kilo pascal (kPa)	1.013 25 X E +2
bar	kilo pascal (kPa)	1.000 000 X E +2
barn	meter^2 (m^2)	1.000 000 X E -28
British thermal unit (thermochemical)	joule (J)	1.054 350 X E +3
calorie (thermochemical)	joule (J)	4.184 000
cal (thermochemical)/cm^2	mega joule/m^2 (MJ/m^2)	4.184 000 X E -2
curie	*giga becquerel (GBq)	3.700 000 X E +1
degree (angle)	radian (rad)	1.745 329 X E -2
degree Fahrenheit	degree kelvin (K)	$t_K = (t°f + 459.67)/1.8$
electron volt	joule (J)	1.602 19 X E -19
erg	joule (J)	1.000 000 X E -7
erg/second	watt (W)	1.000 000 X E -7
foot	meter (m)	3.048 000 X E -1
foot-pound-force	joule (J)	1.355 818
gallon (U.S. liquid)	meter^3 (m^3)	3.785 412 X E -3
inch	meter (m)	2.540 000 X E -2
jerk	joule (J)	1.000 000 X E +9
joule/kilogram (J/kg) (radiation dose absorbed)	Gray (Gy)	1.000 000
kilotons	terajoules	4.183
kip (1000 lbf)	newton (N)	4.448 222 X E +3
kip/inch^2 (ksi)	kilo pascal (kPa)	6.894 757 X E +3
ktap	newton-second/m^2 (N-s/m^2)	1.000 000 X E +2
micron	meter (m)	1.000 000 X E -6
mil	meter (m)	2.540 000 X E -5
mile (international)	meter (m)	1.609 344 X E +3
ounce	kilogram (kg)	2.834 952 X E -2
pound-force (lbs avoirdupois)	newton (N)	4.448 222
pound-force inch	newton-meter (N·m)	1.129 848 X E -1
pound-force/inch	newton/meter (N/m)	1.751 268 X E +2
pound-force/foot^2	kilo pascal (kPa)	4.788 026 X E -2
pound-force/inch^2 (psi)	kilo pascal (kPa)	6.894 757
pound-mass (lbm avoirdupois)	kilogram (kg)	4.535 924 X E -1
pound-mass-foot^2 (moment of inertia)	kilogram-meter^2 (kg·m^2)	4.214 011 X E -2
pound-mass/foot^3	kilogram/meter^3 (kg/m^3)	1.601 846 X E +1
rad (radiation dose absorbed)	**Gray (Gy)	1.000 000 X E -2
roentgen	coulomb/kilogram (C/kg)	2.579 760 X E -4
shake	second (s)	1.000 000 X E -8
slug	kilogram (kg)	1.459 390 X E +1
torr (mm Hg, 0° C)	kilo pascal (kPa)	1.333 22 X E -1

*The becquerel (Bq) is the SI unit of radioactivity; 1 Bq = 1 event/s.
**The Gray (Gy) is the SI unit of absorbed radiation.

TABLE OF CONTENTS

LIST OF ILLUSTRATIONS

I INTRODUCTION

Impact loadings from explosive sources generally deform structural components at high strain rates. These strain rates are manifested via elasto-viscoplastic structural response in many materials such as steel, titanium, and reinforced concrete. It has been shown experimentally that the dynamic load carrying capacities of structures are significantly greater than the corresponding static values. Survey papers of experimental work undertaken to study structural response to impulsive loading have been written by Jones, et. al. [27] and Rawlings [28].

The endeavor to understand and mathematically model the nonlinear, inelastic deformation process has led to various paths of development. From an engineering perspective, concern focuses on establishing techniques which capture the essence of the complex material behavior and are suitable for the analysis of realistically modelled structures. Therefore, this paper discusses the development of an efficient, practical and theoretically sound method of analyzing the dynamic response of structures.

A generalization of the viscoplastic constitutive model as defined by Perzyna [1] has been employed in the formation of a system of equations defining a viscoplastic shell model in the general manner proposed by Bieniek and Funaro [2] for elasto-plastic shells. This resulting shell model is then incorporated into the nonlinear finite difference/finite element code EPSA (Elasto-Plastic Shell Analysis), [3], [4]. The shell model developed in the course of this work utilizes the shell membrane strains and curvatures as the kinematic variables and the shell stress resultants (membrane forces and moments) as the dynamic variables. When compared to the alternative through-the-thickness integration method of calculating stress resultants, this approach offers considerable advantages in terms of both computer storage and speed. Additionally, the model can be fit to experimental data representing various loading combinations (biaxial bending and stretching) at various loading rates on plate and shell specimens.

The shell model approach can also be applied to non-metallic materials. In particular, a reinforced concrete shell model can be formulated, thereby avoiding the difficulties involved in the through-the-thickness approach arising from stress re-distribution due to cracking and debonding.

This paper presents the qualitative and quantitative aspects of the viscoplastic shell model through an examination of a number of multi-dimensional loading combinations at various loading rates for a particular material type. The incorporation of the model into the EPSA code is outlined, and a study is presented of the effects of viscoplastic material response on the dynamic behavior of a cylindrical panel in vacuo and a closed cylinder in an acoustic medium.

It is anticipated that the strain rate-dependent models will be utilized for the analysis of a wide variety of problems of Defense Nuclear Agency interest involving the explosive loading of structures.

II SURVEY OF EXISTING VISCOPLASTIC THEORIES AND THEIR USE IN SHELL ANALYSIS

Continuing research into the viscoplastic behavior of crystalline solids has proceeded from both the microscopic and macroscopic point of view.

Bingham [6] formulated for the case of one dimensional shear a relationship represented by Figure(1). Thic concept was extended to three dimensional states of stress by Hohenemser and Prager [7] with the resulting expression for the plastic strain rate $\dot{\varepsilon}_{ij}^{p}$ in the form

$$\dot{\varepsilon}_{ij}^{p} = \frac{1}{2\mu} \frac{\sqrt{J_2'} - k}{\sqrt{J_2'}} s_{ij} \qquad (1)$$

where J_2' is the second invariant of the deviatoric stress s_{ij}. (μ and k are material constants).

A generalization of these basic ideas has been developed by Perzyna [1]. Included in the specification is the existance of a quasi-static yield function

$$F = \frac{f(\sigma_{ij}, \varepsilon_{ij}^{p})}{\kappa} - 1 \qquad (2)$$

where

$$\kappa = \kappa(W_p) = k \int_0^{\varepsilon_{ij}^{p}} \sigma_{ij} \, d\varepsilon_{ij}^{p} \qquad (3)$$

is the work hardening parameter which describes how the quasi-static yield surface deforms during the inelastic process. The dependence of the plastic strain rate tensor on the stress intensity is given by

$$\dot{\varepsilon}_{ij}^{p} = \gamma\kappa\Phi[F] \frac{\partial f}{\partial \sigma_{ij}} \qquad (4)$$

where γ and $\Phi[F]$ are material response functions. The direction of the viscoplastic strain rate vector is directed along the normal to the subsequent dynamic yield surface.

The dependence of the yield criteria on the strain rate and the dynamic yield criteria for elasto-viscoplastic work-hardening materials is given as

$$f(\sigma_{ij}, \varepsilon_{ij}^{P}) = \kappa(W_p) \left\{ 1 + \Phi^{-1} \left[\frac{(I_2^{P})^{1/2}}{\gamma} \left(\frac{1}{2} \frac{\partial f}{\partial \sigma_{k\ell}} \frac{\partial f}{\partial \sigma_{k\ell}} \right)^{-1/2} \right] \right\} \tag{5}$$

where

$$I_2^{P} = \frac{1}{2} \dot{\varepsilon}_{ij}^{P} \dot{\varepsilon}_{ij}^{P} \tag{6}$$

Figure(2) shows a dynamic stress-strain relation for elastic viscoplastic work-hardening material in simple tension.

A mathematical description of the inelastic metal deformation process proposed by Cernocky and Krempl [8] is based upon the following relation for the plastic strain rates

$$\dot{\varepsilon}_{ij}^{P} = C_{ijk\ell} \frac{\sigma_{k\ell} - G_{k\ell}}{\kappa[\Gamma]} \tag{7}$$

where C_{ijkl} is the elastic compliance tensor, G_{kl} is the stress tensor corresponding to the "equilibrium stress-strain curve", Γ is the second invariant of $(\sigma_{kl} - G_{kl})$ and $\kappa[\Gamma]$ is a material function.

Motivated by dislocation dynamics, Bodner and Partom[9] proposed a functional relationship between the second invariant of the plastic strain rate D_2^p and the second invariant of the deviatoric stress J_2'

$$D_2^p = F[J_2'] \tag{8}$$

where the form of the functional is chosen to reproduce the stress-strain curves of a particular material.

Werne and Kelly [10] arrived at a model of metal viscoplasticity from dislocation dynamics considerations

$$\dot{\varepsilon}_{ij}^{p} = 8b_o \, \beta\eta\xi \, \delta_{ij} \tag{9}$$

where β is a nonlinear function of the deviatoric stress invariant. η and ξ are defined in terms of their evolutionary equations and represent the dislocation density and the mobile fraction, respectively. b_0 is Burger's vector. This model was shown capable of reproducing various types of uniaxial stress-strain curves.

Material models incorporating viscoelastic behavior have also been introduced. Naghdi and Murch [25] have postulated a theory of viscoelastic/plastic solids which reduces to that of linear viscoelasticity and to that of classical plasticity in limiting cases.

Inelastic analysis includes, in addition to a mathematical description of the metal constitutive behavior, a solution scheme for the governing nonlinear equations of motion.

Zirin and Krempl [11] used a finite element technique to solve plane stress, plane strain and axisymmetrical problems incorporating Krempl's [8] viscoplastic model. A particular problem investigated was a thick-walled axisymmetrical cylinder under internal pressure.

Werne and Kelly [10] used the HONDO code [12] response of a cylinder and a bar in uniaxial tension.

A numerical analysis of the elastic viscoplastic response of an axisymmetrical spherical shell was performed by Takezono, et. al. [13] using Perzyna's constitutive model.

The incorporation of the viscoplastic shell model into the EPSA code for usage in solving three dimensional shell type structural problems required the selection of a general form for the viscoplastic constitutive relations. The representation chosen was based upon Perzyna's model [1]. The governing arguments for this selection were:

1. The functional form of the constitutive relations is of sufficient generality so that a broad range of material behavioral patterns could be represented.
2. Experimental verification by Hayashi and Tanimoto[26] of a Perzyna type formulation for describing the response of annealed aluminum to impulsive torque and tension loadings.
3. Retention by the constitutive model of certain basic elements of the classical theory of plasticity which have proved to be a practical and accurate tool of analysis for elasto-plastic structures. In particular, uniqueness arguments of the type made by Drucker[24] are applicable.
4. The model incorporates multi-dimensional stress-strain states including loading and unloading paths.
5. A shell model formulation could be established incorporating the material constitutive equations.
6. A stable solution scheme for the viscoplastic shell equations could be established.
7. The model is effective in capturing complex material behavior while still being cost effective from a computational point of view.

III MATERIAL CONSTITUTIVE EQUATIONS

Perzyna postulated a set of constitutive equations to represent viscoplastic strain hardening behavior for arbitrary loading histories [[1]. Included in this specification is the direction of the viscoplastic strain rate and the magnitude of allowable stress beyond the static yield surface.

The particular case of constitutive relations chosen is that of elastic visco-perfectly plastic material behavior for which the static yield function in stress space is the von Mises yield condition

$$F(s_{ij}) = \frac{1}{2}\frac{s_{ij}\, s_{ij}}{K^2} - 1 \tag{10}$$

where s_{ij} are the deviatoric stresses, $K = \frac{\sigma_o}{\sqrt{3}}$ and σ_o is the uniaxial static yield stress.

The rate of increase of the inelastic components of the strain tensor is a function of the excess stresses beyond the static yield surface(overstress). The direction of the viscoplastic strain rate vector is along the normal to the subsequent loading surface. These relations are mathematically stated as

$$\dot{\varepsilon}_{ij}^{P} = \gamma K \Phi[F(s_{ij})]\,\frac{\partial F}{\partial s_{ij}} = \bar{\lambda}\,\frac{\partial F}{\partial s_{ij}} \tag{11}$$

where γ and $\Phi[F]$ are material functions which can be chosen to represent the results of experimental tests on the dynamic behavior of a particular material. Current available experimental methods consist of one-dimensional stress-strain tests performed using a hydropneumatic machine or a hopkinson bar technique [14].

Figure(3) shows a one dimensional yield stress versus strain rate curve. Manjoine[17] states that this "S" shaped curve is typical of metals tested within a given range of strain rates. The particulars of the curve vary for each material type.

An approximation or fit to this characteristic yield stress versus strain rate curve is made by the following expression

$$\dot{\varepsilon}_{11}^{P} = a_1(F)^{1/n_1} + \frac{a_2(F)^{n_2}}{(F_L - F)^{n_3}} \tag{12}$$

where

$$F_L = \left(\frac{\sigma_L}{\sigma_o}\right)^2 - 1 \tag{13}$$

and σ_L is a limiting one dimensional yield stress achieved from dynamic tests at the highest of strain rates of interest.

Note that equation (12) can be reduced to either a convex or concave power law (with or without an upper limiting stress) representation of the yield stress versus strain rate behavior. The power law representation has been prevalent in previous works [15] and [16].

This one dimensional experimental data can be represented in Perzyna's formulation by assuming $\Phi[F] = F$ and using a suitable functional form for γ. Then, specializing equation (11) to one dimensional behavior

$$\dot{\varepsilon}_{11}^{P} = \frac{2}{\sqrt{3}} \gamma \frac{\sigma_{11}}{\sigma_o} \left(\frac{\sigma_{11}^2}{\sigma_o^2} - 1\right) \tag{14}$$

or in terms of the static yield function $F(\delta_{ij})$

$$\dot{\varepsilon}_{11}^{P} = \frac{2}{\sqrt{3}} \gamma F(\sqrt{F+1}) \tag{15}$$

Equations (12) and (15) state that the material response function γ is

$$\gamma = \frac{\sqrt{3}}{2}\left[\frac{a_1}{(F)^{1-1/n_1}\sqrt{F+1}} + \frac{a_2\,(F)^{n_2-1}}{(F_L - F)^{n_3}\sqrt{F+1}}\right] \tag{16}$$

Appropriate values of the material constants a_1 , a_2 , n_1 , n_2 and n_3 are determined by curve fitting to one dimensional stress-strain rate experimental data.

As an illustrative example, the uniaxial behavior of a mild steel within the strain rate range of $(10)^0$ to $(10)^3$ 1/sec is investigated.

The experimental data of Clark and Duwez [18] is fit to via the parameter values shown in Figure(4).

The general character of equation (16) is that γ approaches infinity at the asymptotes $F = 0$ and $F = F_L$. This behavior can also be represented by the expression

$$\gamma = \frac{\bar{a}_1}{F^{\bar{n}_1}(F_L - F)^{\bar{n}_2}} \tag{17}$$

The curve fit and parameter values using equation(17) are shown in Figure (5) for the mild steel material.

IV SHELL CONSTITUTIVE EQUATIONS

Shell structures resist external loading by developing internal biaxial forces and moments. Two alternative computational approaches for obtaining these internal stress resultants are presented.

a. Through-The-Thickness Integration

For this technique, the time increments of strains at any point of the shell are expressed in terms of the strain and curvature increments of the middle shell surface.

$$\Delta_N \varepsilon_{ij}(z) = \Delta_N \varepsilon_{ij} + \Delta_N \kappa_{ij} Z \tag{18}$$

The time increments of shell forces and moments(stress resultants) are determined by

$$\Delta_N N_{ij} = \int_{-h/2}^{h/2} \Delta_N \sigma_{ij}\, dz \qquad \Delta_N M_{ij} = \int_{-h/2}^{h/2} \Delta_N \sigma_{ij}\, z\, dz \tag{19}$$

The integrals are numerically computed by dividing the shell thickness into "k" layers and assuming a linear stress distribution within each layer.

The stress increments $\Delta_N \sigma_{ij}$ are computed from the material constitutive equations

$$\Delta_N \sigma_{ij} = \sigma_{ij}^{N} - \sigma_{ij}^{N-1} = C_{ijk\ell}\, \Delta_N(\varepsilon_{k\ell} - \varepsilon_{k\ell}^{p}) \tag{20}$$

where σ_{ij}^{N} is the stress tensor after "N" time increments, C_{ijkl} is the elastic moduli matrix. The total strain increment to be separated into elastic and inelastic components.

$$\Delta_N \varepsilon_{ij} = \Delta_N \varepsilon_{ij}^{e} + \Delta_N \varepsilon_{ij}^{p} \tag{21}$$

Equation (20) may be interpreted as

$$\sigma_{ij}^{N} = \sigma_{ij}^{ElTr} - C_{ijk\ell}\, \Delta_N \varepsilon_{k\ell}^{P} \qquad (22)$$

where σ_{ij}^{ElTr} is the stress tensor based upon a trial assumption of total elastic behavior occuring within the N^{th} time step.

$$\sigma_{ij}^{ElTr} = \sigma_{ij}^{N-1} + C_{ijk\ell}\, \Delta_N \varepsilon_{k\ell} \qquad (23)$$

Writing the viscoplastic relations (equation(11)) in time incremental fashion

$$\Delta_N \varepsilon_{ij}^{P} = \Delta t \gamma\, K F(s_{ij}^{N}) \frac{\partial F}{\partial s_{ij}^{N}} = \lambda \frac{\partial F}{\partial s_{ij}^{N}} \qquad (24)$$

λ is a non-negative variable which must be determined as follows;

$$\lambda = \gamma \Delta t K F(s_{ij}^{ElTr} - C_{ijk\ell} \Delta_N \varepsilon_{k\ell}^{P}) \qquad (25)$$

Noting $\frac{\partial F}{\partial s_{ij}^{N}} = \frac{s_{ij}}{K^2}$ and $C_{ijk\ell} s_{k\ell} = 2G\, s_{ij}$, Equation (25) becomes,

$$\lambda = \gamma \Delta t K F(s_{ij}^{ElTr} - \frac{2G\lambda}{K^2} s_{ij}) \qquad (26)$$

Equating arguments of function $F(s_{ij})$ yields,

$$s_{ij} = \frac{s_{ij}^{ElTr}}{1 + \frac{2G}{K^2}\lambda} \qquad (27)$$

and

$$\lambda = \gamma \Delta t K \left(\frac{\frac{1}{2} s_{ij}^{ElTr} s_{ij}^{ElTr}}{(1 + \frac{2G}{K^2}\lambda)^2 K^2} - 1 \right) \qquad (28)$$

Rearranging equation (28) gives

$$\left(\frac{4G^2}{K^2}\right) \lambda^3 + \left(\frac{4G}{K^2} + \frac{4G^2 \gamma \Delta t}{K^3} \right) \lambda^2 + \left(1 + \frac{4G\gamma\Delta t}{K}\right) \lambda - \gamma \Delta t K \left(F(s_{ij}^{ElTr})\right) = 0 \qquad (29)$$

The real root is extracted from a cubic equation solver of $\lambda[\gamma, \Delta t, K, G, F(\sigma_{ij}^{ElTr})] = 0$ where γ is given as described in Section III.

b. <u>Viscoplastic Shell Model - Direct Formulation</u>

The direct shell model formulation relates the dynamic variables S_{ij} (membrane forces and bending moments) to the kinematic variables e_{ij} (strains and curvatures of the shell's middle surface

$$e_{ij} = \begin{Bmatrix} \varepsilon_{11} \\ \varepsilon_{22} \\ 2\varepsilon_{12} \\ \kappa_{11} \\ \kappa_{22} \\ 2\kappa_{12} \end{Bmatrix} \qquad S_{ij} = \begin{Bmatrix} N_{11} \\ N_{22} \\ N_{12} \\ M_{11} \\ M_{22} \\ M_{12} \end{Bmatrix} \tag{30}$$

The quasi-static yield surface in stress resultant space is

$$F(S_{ij}) = I_N + I_N^2 - I_N^3 + I_M^* + 0.8|I_{NM}| \tag{31}$$

which describes the current yield surface as the loading path moves from an initial yield surface $F_o(S_{ij})$ towards the limit surface $F_L(S_{ij})$.

$$F_o(S_{ij}) = I_N + I_M + 2\,|I_{NM}| \tag{32}$$

$$F_L(S_{ij}) = 2\,I_N - I_N^2 + \frac{4}{9}\,I_M \tag{33}$$

where I_N, I_M, I_{NM} and I_M^* are stress resultant invariants defined as

$$I_N \equiv \frac{1}{N_0^2}(N_{11}^2 + N_{22}^2 - N_{11}\,N_{22} + 3\,N_{12}^2)$$

$$I_M \equiv \frac{1}{M_0^2}(M_{11}^2 + M_{22}^2 - M_{11}\,M_{22} + 3\,M_{12}^2)$$

$$I_{NM} \equiv \frac{1}{N_0 M_0}(N_{11}\,M_{11} + N_{22}M_{22} - \frac{1}{2}\,N_{11}M_{22} - \frac{1}{2}\,N_{22}M_{11} + 3\,N_{12}M_{12})$$

$$I_M^* = \frac{1}{M_0^2}[(M_{11} - M_{11}^*)^2 + (M_{22} - M_{22}^*)^2 \tag{34}$$

$$- (M_{11} - M_{11}^*)(M_{22} - M_{22}^*) + 3(M_{12} - M_{12}^*)^2]$$

and

$$N_0 = \sigma_0 h \quad , \quad M_0 = \sigma_0 h^2/6$$

where σ_o is the static yield strength.

The quantities M_{ij}^*, which will be referred to as " hardening parameters " are defined by

$$\text{If } F = 1 \text{ and } \frac{\partial F}{\partial N_{ij}} \dot{N}_{ij} + \frac{\partial F}{\partial M_{ij}} \dot{M}_{ij} > 0: \quad dM_{ij}^* = \beta_{ij}(1-F_L) \frac{M_o}{\kappa_o} \partial\kappa_{ij}^p$$

$$\text{If } F < 0 \text{ or } \frac{\partial F}{\partial N_{ij}} \dot{N}_{ij} + \frac{\partial F}{\partial M_{ij}} \dot{M}_{ij} \leq 0: \quad dM_{ij}^* = 0 \tag{36}$$

The elastic law

$$S_{ij} = E_{ijk\ell}(e_{k\ell} - e_{k\ell}^p) \tag{37}$$

is used where E_{ijkl} is the elastic shell stiffness matrix.

The above quasistatic shell formulation is derived from that proposed by Bieniek and Funaro [2] for elasto-plastic shell analysis Alterations have been made in the specification of the variable yield surface, the limit surface, and the hardening law, resulting in a more accurate representation of the quasistatic elasto-plastic shell behavior. In order to generalize the model to include strain rate effects along the lines of equation (11), the plastic strain rate tensor is assumed to depend on the stress resultant intensity through the associated flow rule

$$\dot{e}_{ij}^p = \gamma_R K\, \Phi[F(S_{ij})]\, \frac{\partial F(S_{ij})}{\partial S_{ij}} = \bar{\lambda}\, \frac{\partial F(S_{ij})}{\partial S_{ij}} \tag{38}$$

Recalling the work of section III, one obtains

$$\lambda = \gamma_R \Delta t K\, F(S_{ij}^{ElTr} - E_{ijk\ell}\, \lambda \frac{\partial F}{\partial S_{k\ell}}) \tag{39}$$

Because equation (39) cannot be solved in closed form for λ, the equivalent form

$$\lambda[\gamma_R, \Delta t, K, E_{ijk\ell}, F(S_{ij}^{ElTr}), \frac{\partial F}{\partial S_{ij}}] = 0 \tag{40}$$

is solved iteratively using a modified regula falsi method.

γ_R is a physical function which should be chosen to represent the results of multiaxial tests on plate and shell specimens of a particular material. These experiments should consist of biaxial bending and stretching tests conducted at various loading rates of concern. The present lack of such experimental data precludes the possibility of choosing this function to fit measured results. Therefore, at this time, γ_R will be chosen such that the produced stress resultants obtained via the proposed viscoplastic shell model satisfactorily represent those obtained using the through-the-thickness approach for various loading paths.

For the mild steel material [18], previously discussed, the proposed form of the function γ_R is

$$\gamma_R = \frac{\bar{A}_1[I_N, I_M^*]}{(F_R)^{\bar{n}_1} (1 - (\frac{\sigma_o}{\sigma_L})^2 F_R)^{\bar{n}_2}} \tag{41}$$

where

$$\bar{A}_1[I_N, I_M^*] = A_1(\frac{I_N + A_2A_3 I_M^*}{I_N + A_3I_M^*}) \tag{42}$$

and

$$F_R = C_1(I_N + I_N^2 - I_N^3) + C_2(I_M^*) + C_3|I_{NM}| \tag{43}$$

This formulation respresents an eight parameter model $\bar{n}_1$, $\bar{n}_2$, A_1 , A_2 , A_3 , C_1 , C_2 , C_3) whose values are chosen such that the viscoplastic shell model results correspond to the calculated through-the-thickness viscoplastic shell behavior for various loading rates and paths for the mild steel specimens. A discussion of the determination of these parameters will be given in Section V.

V COMPARISON OF THROUGH-THE-THICKNESS AND SHELL MODEL RESULTS FOR THE BEHAVIOR OF MILD STEEL

Multi-dimensional structural response involves the determination of biaxial shell forces and moments for various combinations of induced axial and bending strains. With this is mind, a series of loading cases is introduced , with each case reflecting a particular stress state feature. Figure (6) presents a listing of particular loading cases considered.

Continuing the illustrative example of mild steel behavior, the viscoplastic shell model parameters of equations (42) and (43) were determined such that the shell model results matched the through-the-thickness results for the loading paths listed in Figure (6) for loading rates $(10)^0$ to $(10)^3$ 1/sec.

For the mild steel considered, the determined material constants are

$$\bar{n}_1 = 3/4 \qquad \bar{n}_2 = 1/4$$

$$A_1 = 20.0 \qquad A_2 = 1.0 \qquad A_3 = 1.0$$

$$C_1 = 1.0 \qquad C_2 = 0.4 \qquad C_3 = 0.8$$

For the loading cases analyzed, various features of the viscoplastic shell behavior are presented in Figures(7) to (23).

Figure (7) shows the variability in the axial force as a function of the applied strain rate. An increase of the yield force is seen for increasing strain rates and a corresponding reduction in yield force for decreasing strain rates. It is seen that a rise in the strain rate raises the flow stress rapidly from its previous stationary value and as straining continues at the more rapid rate, the stress approaches the value it would have had if the entire straining process was performed at this rapid strain rate. Thus, the effects of strain rate history are erased. Experimentally, it has been shown [19] that for mild steel, strain rate history effects are minimal at ambient temperatures.

For the viscoplastic shell behavior in one dimensional bending, Figure (8) presents the moment-curvature diagrams for various loading rates. Figure (9) shows the increase of the limit force and the limit moment due to strain rate effects. One notices in Figure (9) that, at a particular loading rate, the limit moment is not as dynamically enhanced as the limit force. This is due to the variability in the strain rates through-the-thickness of the shell when deforming in a bending mode.

Loading cases three through six represent a variety of biaxial stress resultant states dominated by a particular force and/or moment. Various radial loading paths of stretching ($\Delta\varepsilon$) and bending ($\Delta\kappa$) strain increments were prescribed to produce the biaxial stress resultant states $N_1 = N$, $N_2 = \alpha N$, $M_1 = M$ and $M_2 = \beta M$. These loading cases were investigated for loading rates varying from $(10)^0$ to $(10)^3$ 1/sec. For the sake of brevity, the loading rate of 120 1/sec is chosen to illustrate the shell model's applicability. Each of the featured cases consists of a cyclic loading curve. The viscoplastic shell model captures the essential features and characteristics of the through-the-thickness integration calculations, as shown in Figures (10) to (14) .

Figures (15) to (18) illustrate the variability in the stress resultant limit state for the condition of equal biaxial forces and equal biaxial moments. The ratio of stretching ($\Delta\varepsilon$) to bending ($\Delta\kappa$) is varied to produce various combinations of forces and moments. It is clear that the viscoplastic shell model produces a very good definition of the effect of strain rates on the dominating stress resultant quantities. The existing small deviations are seen to be independent of the loading rate and are therefore due to approximations inherent in the specification of the quasi-static yield surface.

Loading cases eight through twelve represent equal absolute magnitude biaxial forces and biaxial moments, with differing signs. Figures (19) through (23) illustrate these cases and show the good agreement which exists.

Therefore, for the various loading combinations which can occur in shell structures, it is shown that the model provides a very good definition of the viscoplastic shell behavior as determined by the through-the-thickness integration procedure. The selection of suitable but different model parameters should provide the same favorable approximations for other structural metals.

When biaxial experimental data becomes available, the model parameters can be fit to the data. It has been shown that for dynamic one dimensional bending, deviations do exist between measured moments and those computed using the through-the-thickness integration technique[20].

VI INCORPORATION OF VISCOPLATIC MODEL INTO EPSA CODE

The EPSA [3] code has been developed for the dynamic response analysis of stuctures in an acoustic medium , including both plastic collapse and/or local instability (dynamic buckling) of the structure. The following is a brief description of the theoretical basis of the code:

The structural equations of motion are derived for the principle of virtual work

$$\int_R \{S\}^T\{\delta e\}dR - \int_R \{P\}^T\{\delta u\}\, dR + \int_R \rho\{\ddot{u}\}\{\delta u\}\, dR = 0 \qquad (44)$$

with $\{u\} = (u_1, u_2, w)^T$

A finite difference / finite element method is used to discretize the non-linear equations of motion. The surface of the region R is covered with a quadrilateral mesh of "j" elements, each element of area A_i.

Each arbitrarily shaped quadrilateral shell element is defined by four corner nodes, with each node having three translational and no rotational degrees of freedom. Spacial derivatives are expressed in terms of discrete nodal displacements via an irregular finite difference technique. A two dimensional Taylor series expansion in irregularly shaped meshes is employed [5]].

The integrals over region R of equation (44) are replaced by sums of integrals over A_i to obtain the following system of ordinary differential equations:

$$[M]\,\{\ddot{q}\} = \sum_{i=1}^{j} [\{P\}_i - \{F\}_i] \qquad (45)$$

where {q} is the nodal displacement vector for the structure, [M] is the lumped mass matrix ,{P} represents the vector of external forces acting on the nodes of the structure, {F} is the vector of equivalent internal grid point forces.

The system of equations for the nodal displacements is integrated in time using an explicit central difference scheme.

The Donnell-Vlasov nonlinear kinematic equations of shell theory are used. The geometric nonlinearities are accounted for in the strain - displacement relations

$$\{\dot{e}\} = [B]\ \{\dot{q}\} \tag{46}$$

The viscoplastic shell equations relate the stress resultant vector to the shell strain rate vector. These equations are solved at each time step. The magnitude of the time step is governed by the Courant criterion for the integration of the spatially discretized equations of motion.

The use of the viscoplastic shell theory results in an increase in the efficiency of the computational procedure as compared to the through-the-thickness integration technique. This occurs because the shell theory employs nine memory parameters per element versus the 42 (6 * Number of Layers) quantities for the through-the-thickness technique. Also, the solution procedure for the shell model requires approximately 50% less computer time than the through-the-thickness technique.

VII VISCOPLASTIC SHELL ANALYSIS USING EPSA

REPRESENTATIVE EXAMPLES

The EPSA code with the inclusion of a viscoplastic shell model was used to investigate the elastic viscoplastic, large deflection, transient response of shell structures.

An analysis was performed to determine the response of a clamped-edge, mild steel, cylindrical panel subjected to impulsive loading by the sheet explosive loading technique. The geometric properties of the panel are shown in Figure (24).

Analysis of the structure by EPSA consisted of a one hundred element mesh configuration for the quarter model, Figure (25). Initial conditions consist of initial radial velocities obtained by equating the impulse imparted by the detonated sheet to the total impulse experienced by the structure.

Figures (26) and (27) illustrate the results of two EPSA analyses, one using an elasto-plastic shell model (quasi-static yield strength), the other using a viscoplastic shell model. The viscoplastic material effects are shown to reduce the permanent deflection at the center of the specimen by twenty five percent. The peak inner fiber circumferential strain at the mid-point of the specimen is reduced from 3 percent to 2 percent due to viscoplastic shell behavior.

The second example investigated involved a stiffened cylindrical shell immersed in an acoustic medium subjected to shock loading, Figure (28). The pressure function contains an exponential decay in time and a linear spatial decay.

The EPSA quarter model of the shell and internal stiffeners consists of a 1440 element mesh. The fluid/structure interface is accounted for by means of the Doubly Asymptotic Approximation [23].

Again, two distinct EPSA analyses were performe to isolate the effects of strain rate behavior upon the calculated response of the structure. Figure (29) shows the calculated deflection pattern across the length of the shell at the circumferential zero degree line (initial load impact position) fot the two analyses. The variability in the inner fiber circumferential strains at Frame 5 1/2 at zero degrees and 180 degrees is shown in Figure (30) for the two analyses.

VIII CONCLUSIONS

An analysis method is presented for obtaining the dynamic response of elasto-viscoplastic structures. This technique consists of the development of a viscoplastic shell theory and its incorporation into the EPSA code. The effects of viscoplastic material behavior upon the response of structures in vacuo or in an acoustic medium when subjected to transient loadings is demonstrated.

Viscoplastic material response is shown to significantly increase the resistance of shells to dynamic loadings.

Continuing development work can encompass the following:

1. Employ the proposed method to analyze the viscoplastic response of mild steel frame, plate and shell specimens and compare to available experimental data, [21],[22].
2. Fit the shell model parameters to additional material types, i.e., titanium and high strength steels.
3. Incorporate strain hardening into the material constitutive equations.
4. Explore the possibility of obtaining experimental biaxial stress resultants versus strain rate data so that the viscoplastic shell model parameters can be fit to such data rather than to the through-the-thickness results.

REFERENCES

1. Perzyna, P., "Fundamental Problems in Viscoplasticity", Advances in Applied Mechanics, Vol. 9, 1966, Academic Press, pp. 243-377.

2. Bieniek, M.P. and Funaro, J.R., "Elasto-Plastic Behavior of Plates and Shells", Report No. DNA 3954T, Weidlinger Associates, New York, New York, March 1976.

3. Atkatsh, R., Bieniek, M.P. and Baron, M.L., "Dynamic Elasto-Plastic Response of Shells in an Acoustic Medium-Theoretical Development for the EPSA Code", Technical Report No. 24, ONR Contract Nos. N00014-72-C-0119 and N00014-78-C-0820, Weidlinger Associates, New York, New York, July 1978.

4. Atkatsh, R., Daddazio, R.P., "Dynamic Elasto-Plastic Response of Shells in an Acoustic Medium - Users Manual for the EPSA Code", Technical Report No. 27, ONR Contract No. N00014-78-C-0820, Weidlinger Associates, New York, New York, March 1980.

5. Atkatsh, R., Bieniek, M.P. and Baron, M.L., "A Finite Difference Method for Bending of Plates", Computers and Structures, Vol. II, pp. 573-577, 1980.

6. Bingham, E.D., "Fluidity and Plasticity", McGraw-Hill, 1922.

7. Hohenemser, K., and Prager, W.,, Über die Ansätze der Mechanik isotroper Kontinua, Zeitschrift F. agnew. Math. U. Mech. 12, 216-226, 1932.

8. Cernocky, E.P. and Krempl, E., "A Theory of Viscoplasticity based on Infinitesimal Total Strain", ACTA Mechanica, Vol. 36, pp. 263-289, 1980.

9. Bodner, S.R. and Partom, Y., "Constitutive Equations for Elastic-Viscoplastic Strain-Hardening Materials", J. Appl. Mech., June 1975, pp. 385-389.

10. Werne, R.W. and Kelly, J.M., "Rate Dependent Inelastic Behavior of Polycrystalline Solids using a Dislocation Model", Century 2 Pressure Vessels and Piping Conference, ASME, 1980.

11. Zirin, R.M. and Krempl, E., "A Finite Element Time Integration Method for the Theory of Viscoplasticity Based on Infinitesimal Total Strain" Century 2 Pressure Vessels and Piping Conference, ASME, 1980.

12. Key, S.W., "HONDO - A Finite Element Computer Program for the Large Deformation Dynamic Response of Axisymmetric Solids", SLA 74-0039, 1974, Sandia Laboratories, Albuquerque, New Mexico.

13. Takezono, S., Tao, K., Kanezaki, K., "Elasto/Viscoplastic Dynamic Response of Axisymmetrical Shells by Overlay Model", Journal of Pressure Vessel Technology, Vol. 102, pp. 257-263, August 1980.

14. Lindholm, U.S., "Review of Dynamic Testing Techniques and Material Behavior", Conference on Mechanical Properties of Materials at High Rates of Strain, Institute of Physics, London, 1974.

15. Perrone, N., "Response of Rate Sensitive Frames to Impulse Load", Journal of Engineering Mechanics, ASCE, Feb. 1971, pp. 49-62.

16. Symonds, P.S. and Chon, C.T., "Large Viscoplastic Deflections of Impulsively Loaded Plane Frames", Brown University, Report N000014-0860/3, Sept. 1977.

17. Manjoine, M.J., "Effect of Rate of Strain on the Flow Stress of Gas Turbine Alloys at 1200 and 1500 F.", Proc. Amer. Soc. Testing Materials, Vol. 50, pp. 931-947, 1950.

18. Clark, D.S. and Duwez, P.E., "The Influence of Strain Rate on Some Tensile Properties of Steel", Proc. Amer. Soc. Testing Materials, Vol. 50, pp. 560-575, 1950.

19. Klepaczko, J. and Duffy, J., "Strain Rate History Effects in BCC Metals", Brown University Report MRLE-128, February 1981.

20. Aspden, R.J. and Campbell, J.D., "The Effect of Loading Rate on the Elasto-Plastic Flexure of Steel Beams", Proceedings of the Royal Society, Volume A290, pp. 266-285, 1966.

21. Jones, N., Uran, T.O. and Tekin, S.A., "The Dynamic Plastic Behavior of Fully Clamped Rectangular Plates", Int. J. Solids and Structures, Vol. 6, pp. 1499-1512, 1970.

22. Bodner, S.R. and Symonds, P.S., "Experiments on Viscoplastic Response of Circular Plates to Impulsive Loading", Brown University, Report N00014-0860/6, July 1977.

23. Geers, T.L., "Residual Potential and Approximate Method for Three-Dimensional Fluid-Structure Interaction Problems", J. Acoust. Soc. Amer., Vol. 49, No. 5, Part 2, 1971, pp. 1505-1510.

24. Drucker, D., "On Uniqueness in the Theory of Plasticity", Q. Appl. Math, Vol. 14, pp. 35-42, 1956.

25. Naghdi, P.M. and Murch, S.A., "On the Mechanical Behavior of Visco-elastic/Plastic Solids", Journal of Applied Mechanics, Vol. 30, pp. 321-327, 1963.

[26] Hayashi, T. and Tanimoto, N. "Behavior of Materials under Dynamic Combined Stresses of Torsion and Tension:, IUTAM Symposium "High Velocity of Solids", Springer-Verlag N.Y. 1978.

[27] Jones, N., Dumas, J., Grannotti, J. and Grassit, K., MIT Report No. 71-6, 1971.

[28] Rawlings, B., "Response of Structures to Dynamic Loads", Conference of Mechanical Properties of Materials at High Rates of Strain, Institute of Physic, London, 1974.

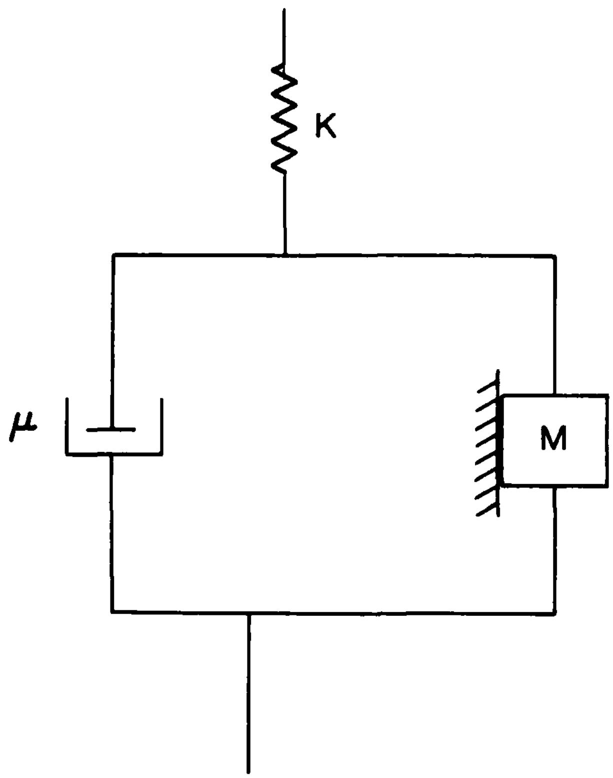

BINGHAM'S
ONE-DIMENSIONAL VISCOPLASTIC MODEL

FIG. 1

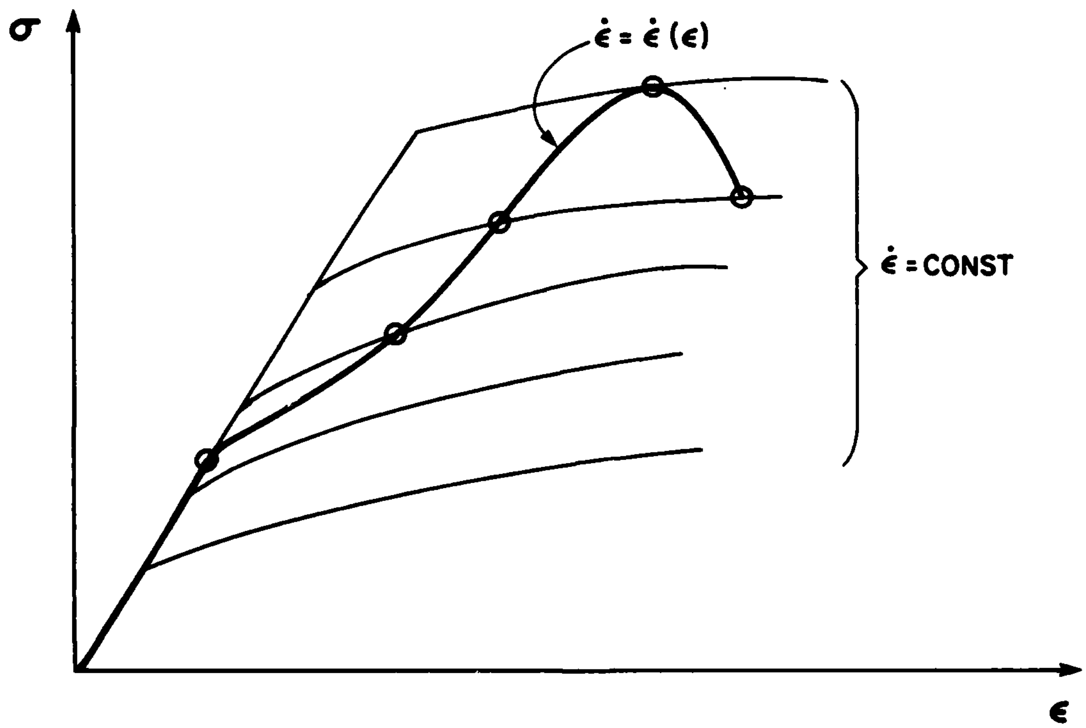

DYNAMIC STRESS-STRAIN RELATION
ELASTIC VISCOPLASTIC MATERIAL
TENSION BEHAVIOR

FIG. 2

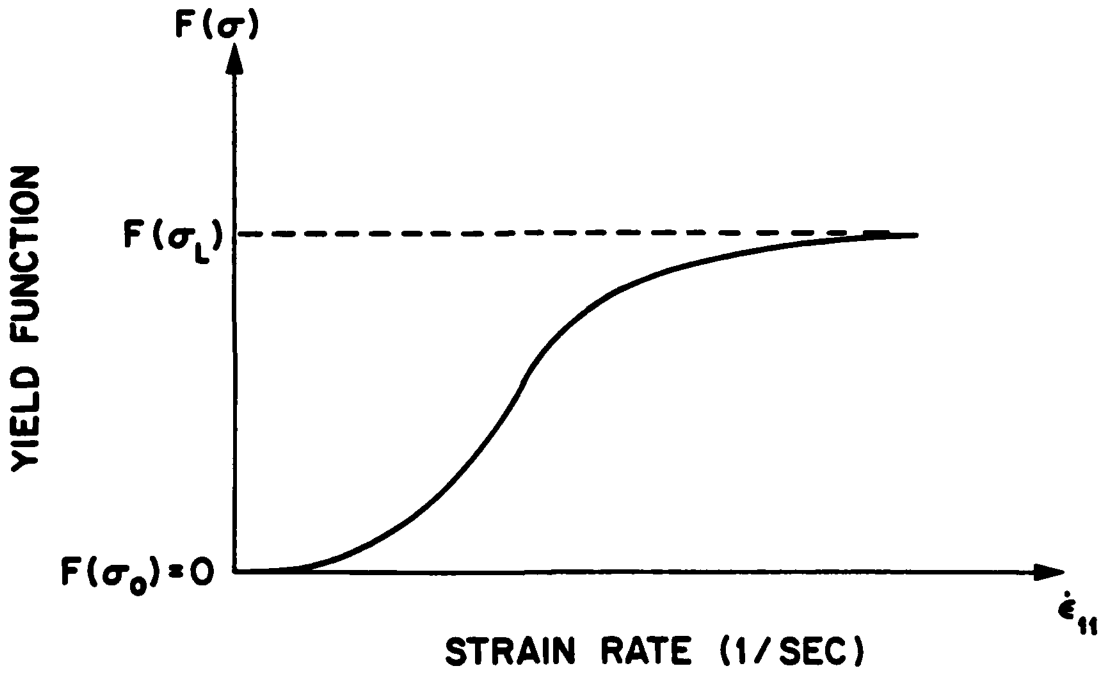

1-D YIELD FUNCTION VS. STRAIN RATE
TYPICAL BEHAVIOR FOR MILD STEEL

FIG. 3

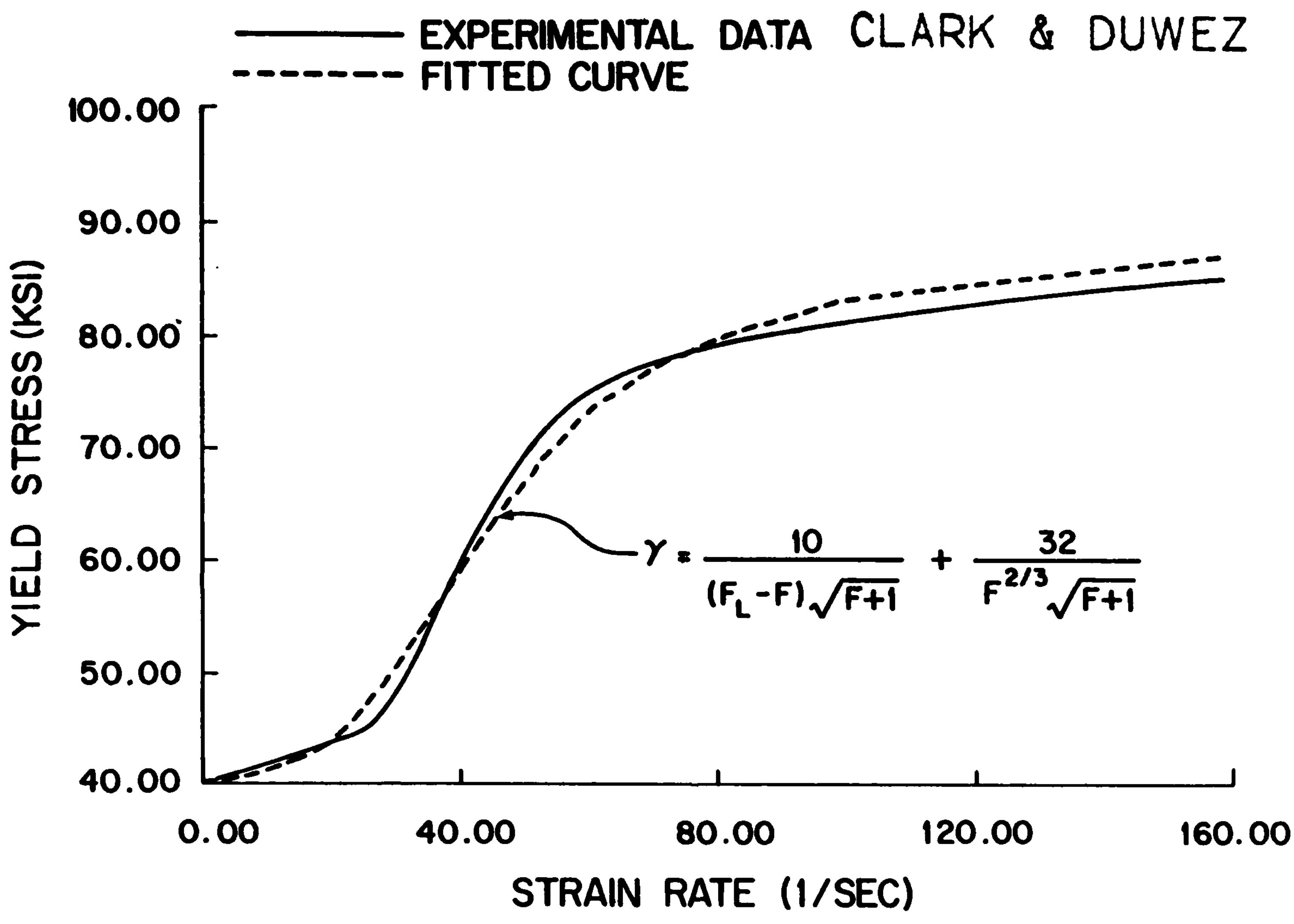

1-D YIELD STRESS VS. STRAIN RATE
MILD STEEL

FIG. 4

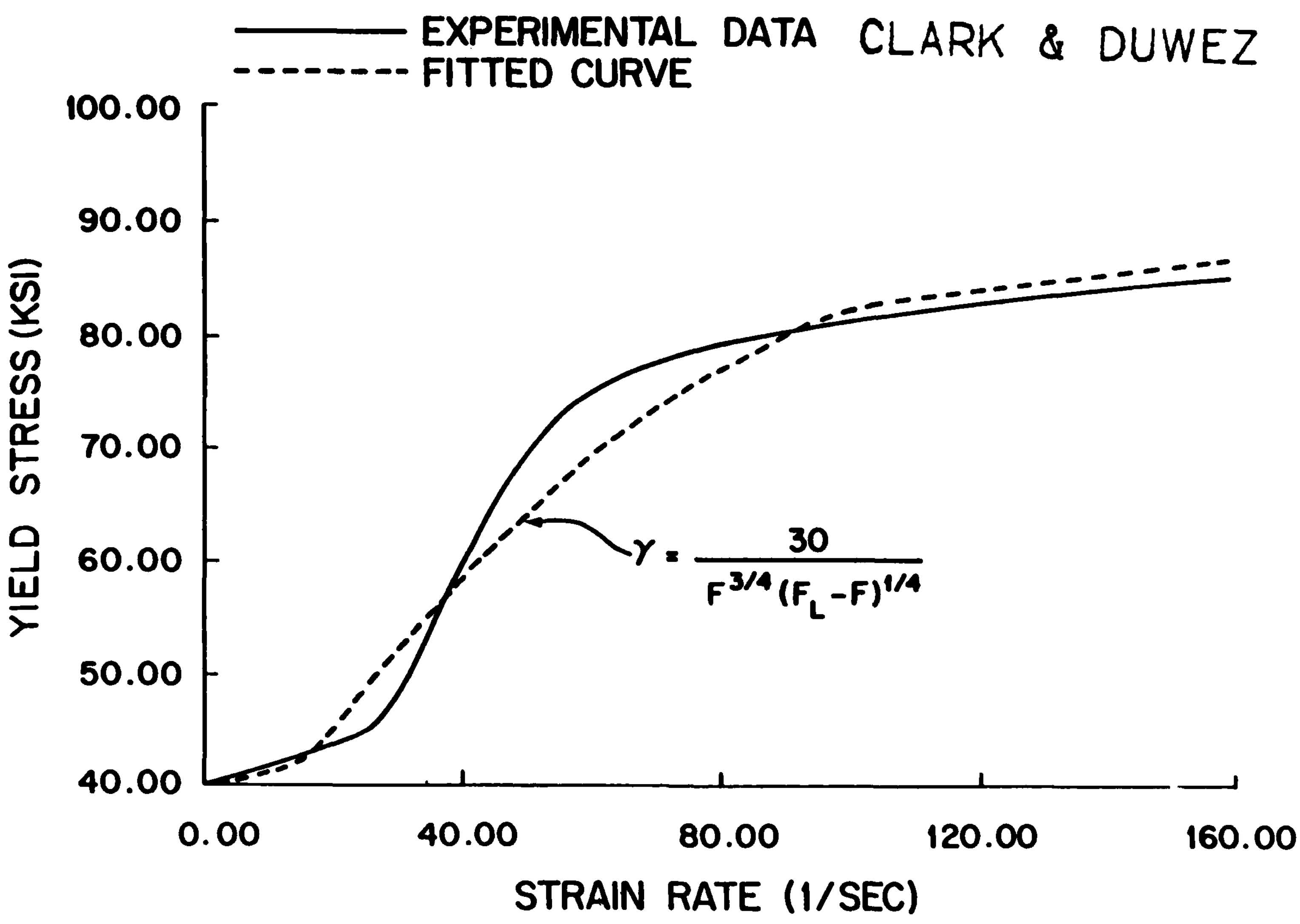

1-D YIELD STRESS VS. STRAIN RATE
MILD STEEL

FIG. 5

MULTI-DIMENSIONAL LOADING PATHS CHOSEN FOR DETERMINATION OF VISCOPLASTIC SHELL MODEL PARAMETERS

LOADING CASE	STRESS RESULTANTS N_1	N_2	M_1	M_2	LOADING DESCRIPTION
1	N	0	0	0	1-D FORCE
2	0	0	M	0	1-D MOMENT
3	0	0	M	βM	2-D MOMENT
4	N	αN	M	βM	M_1 DOMINATES
5	N	αN	M	βM	N_1, M_1 DOMINATE
6	N	αN	M	βM	N_1, M_2 DOMINATE
7 THRU 12	N	±N	M	±M	FORCES OF EQUAL MAGNITUDE MOMENTS OF EQUAL MAGNITUDE

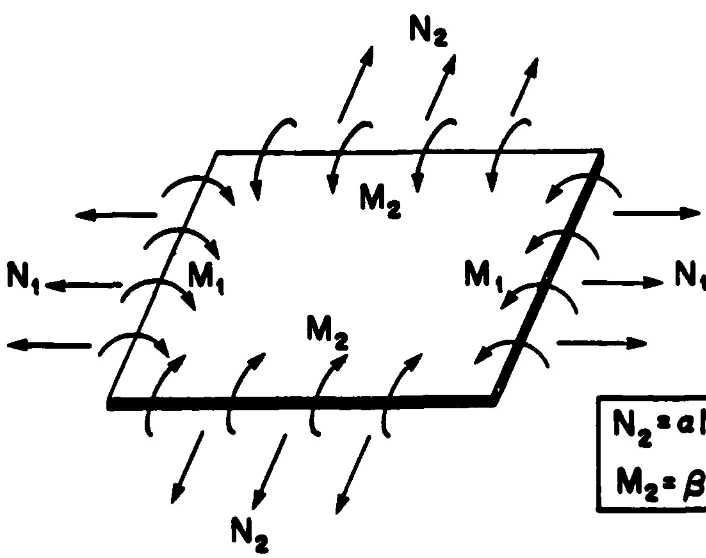

$N_2 = \alpha N_1$
$M_2 = \beta M_1$

FIG. 6

LOADING CASE No. 1

N_1	N_2	M_1	M_2
N	O	O	O

1-D FORCE

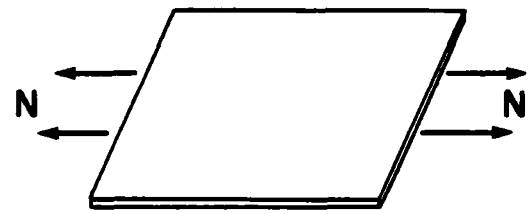

N_0, ϵ_0: STATIC YIELD FORCE AND STRAIN

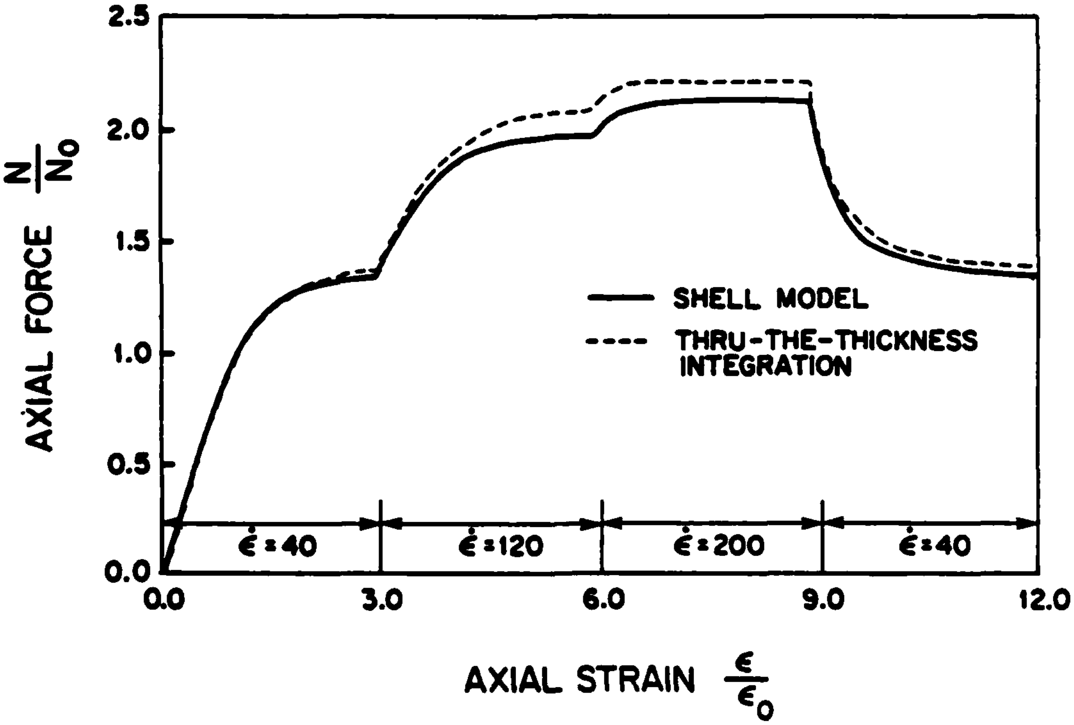

1-D FORCE VS. STRAIN FOR $\dot{\epsilon} = \dot{\epsilon}(\epsilon)$

FIG. 7

LOADING CASE No. 2

1-D MOMENT

N_1	N_2	M_1	M_2
0	0	M	0

M_0, κ_0: STATIC YIELD MOMENT AND CURVATURE

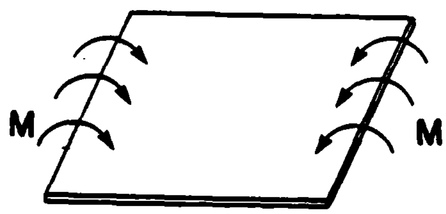

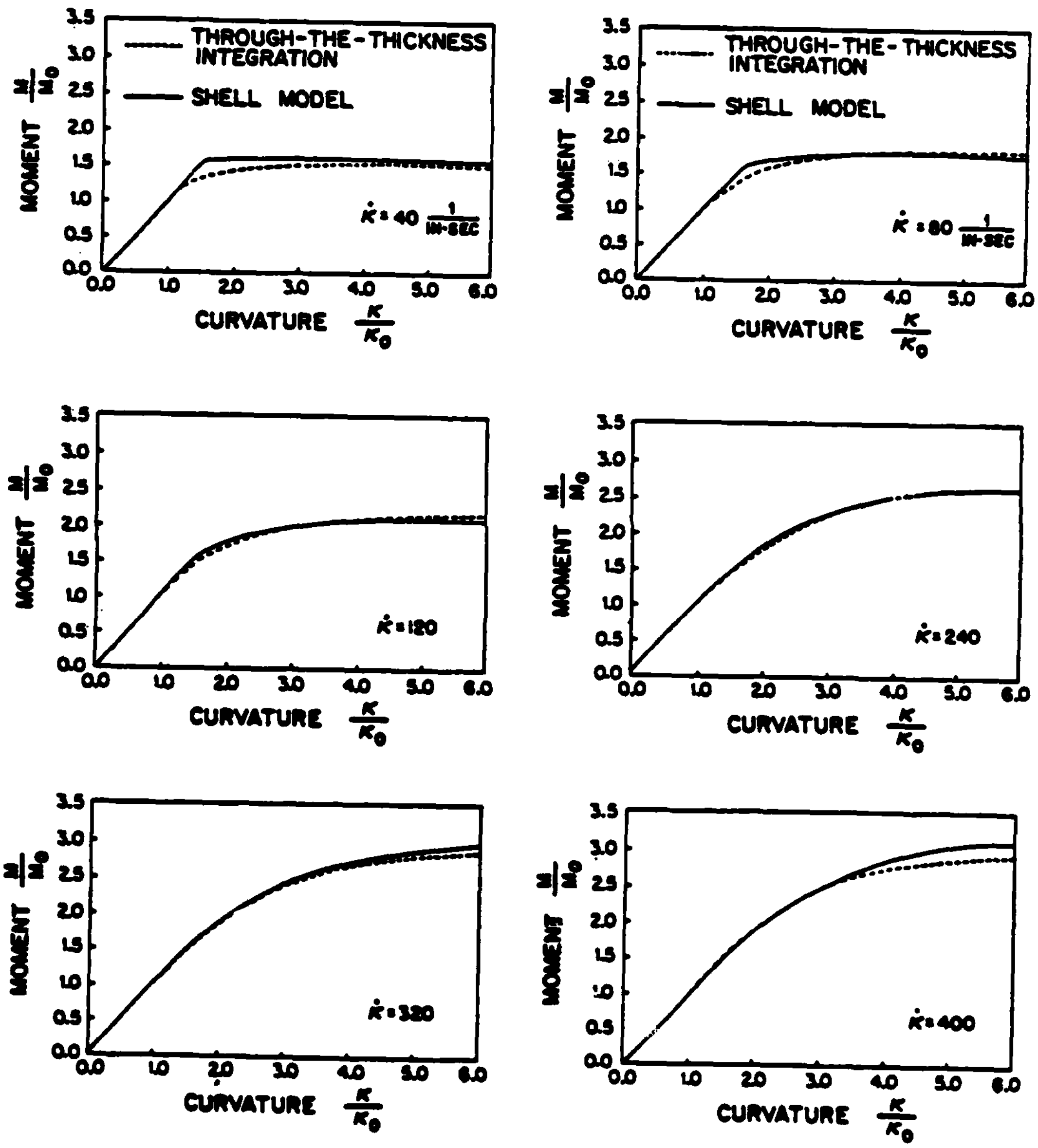

VISCOPLASTIC MATERIAL BEHAVIOR
1-D MOMENT VS. CURVATURE FOR VARIOUS LOADING RATES

FIG. 8

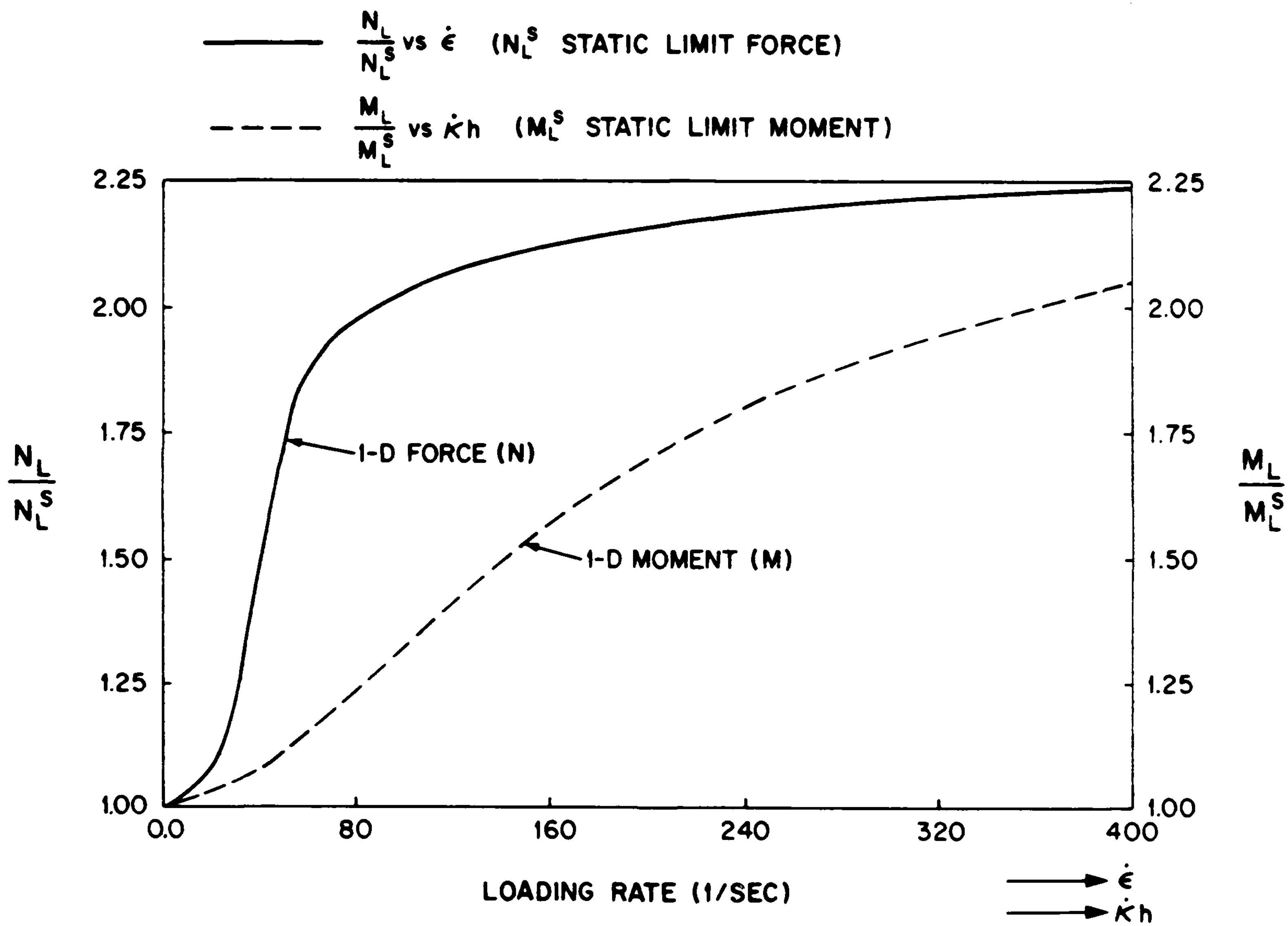

ONE DIMENSIONAL LIMIT FORCE AND MOMENT VS. LOADING RATE

FIG. 9

LOADING CASE No. 3 BIAXIAL MOMENT

N_1	N_2	M_1	M_2
0	0	M	βM

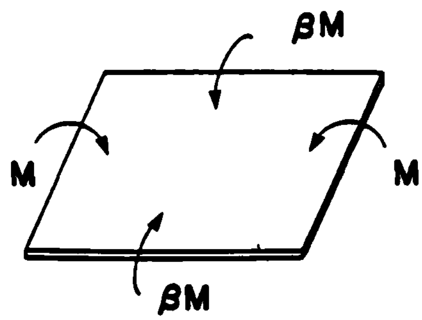

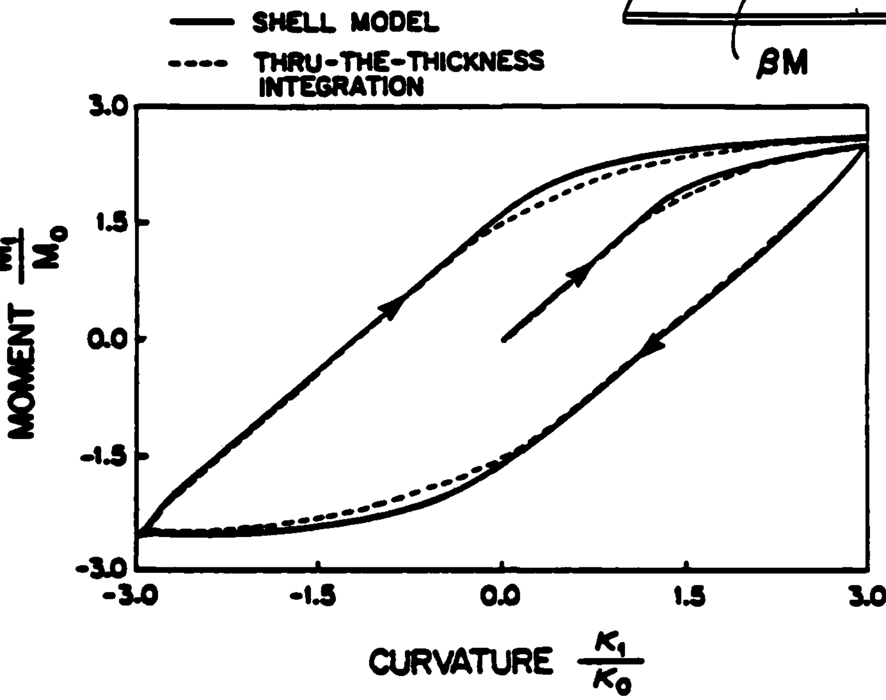

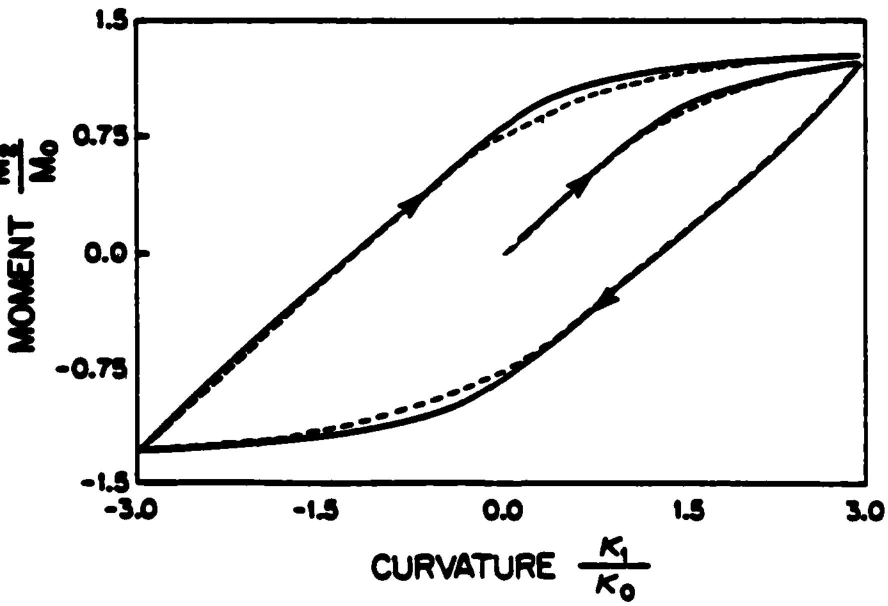

VISCOPLASTIC SHELL BEHAVIOR

MOMENT VS. CURVATURE $\dot{\kappa}_1 = 120$ 1/in·sec

FIG. 10

LOADING CASE No. 4

N_1	N_2	M_1	M_2
N	αN	M	βM

M_1 DOMINATES

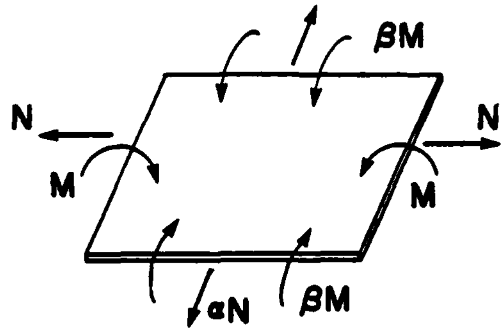

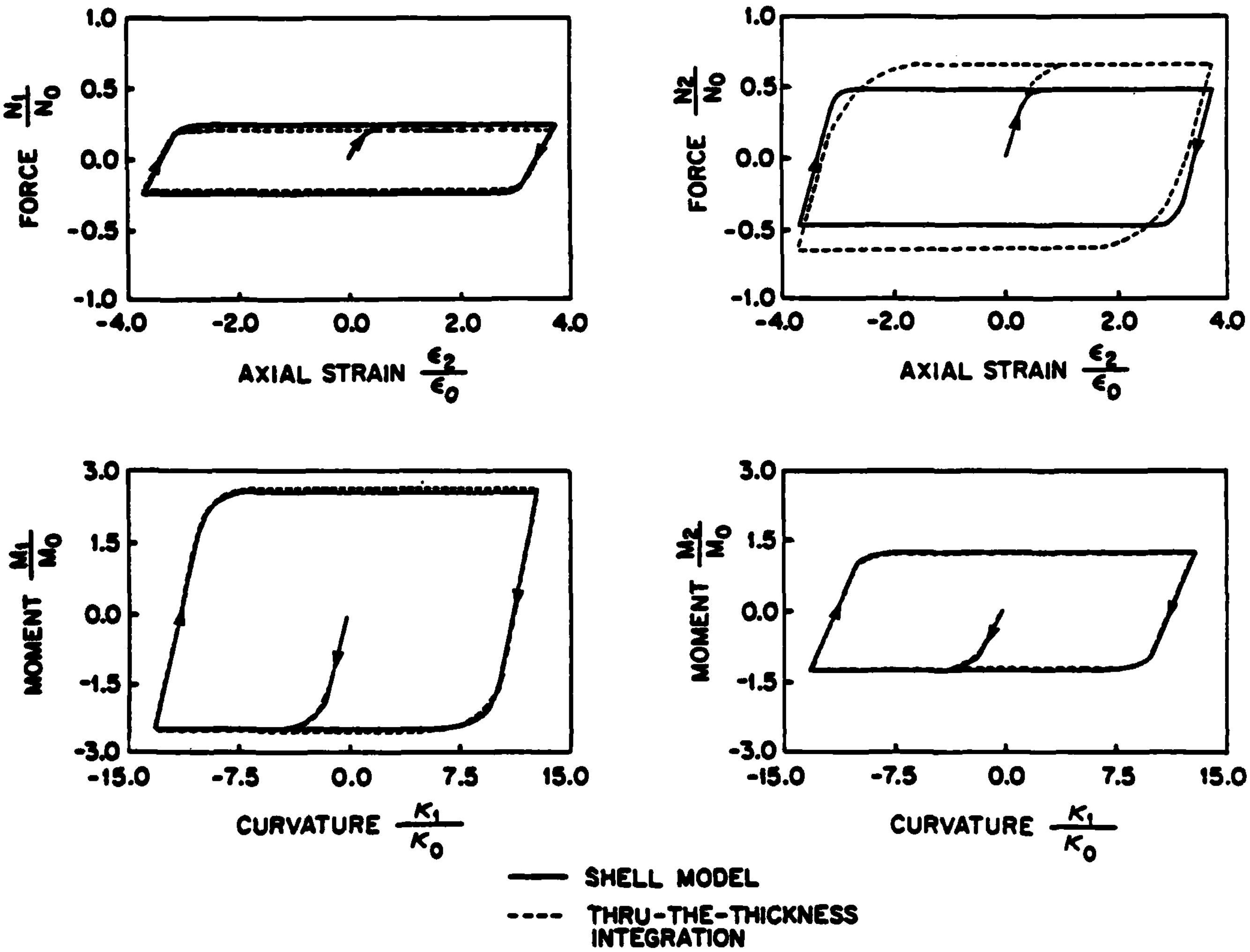

VISCOPLASTIC SHELL BEHAVIOR

LOADING RATE = 120 1/SEC

FIG. 11

LOADING CASE No. 5a

N_1	N_2	M_1	M_2
N	αN	M	βM

N_1, M_1 DOMINATE

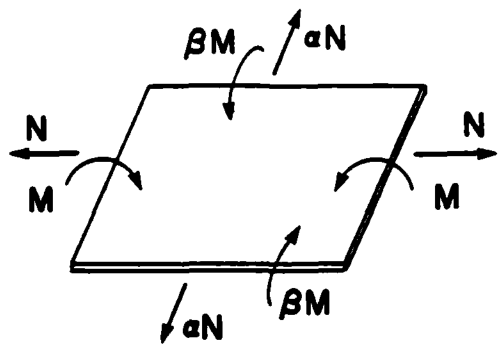

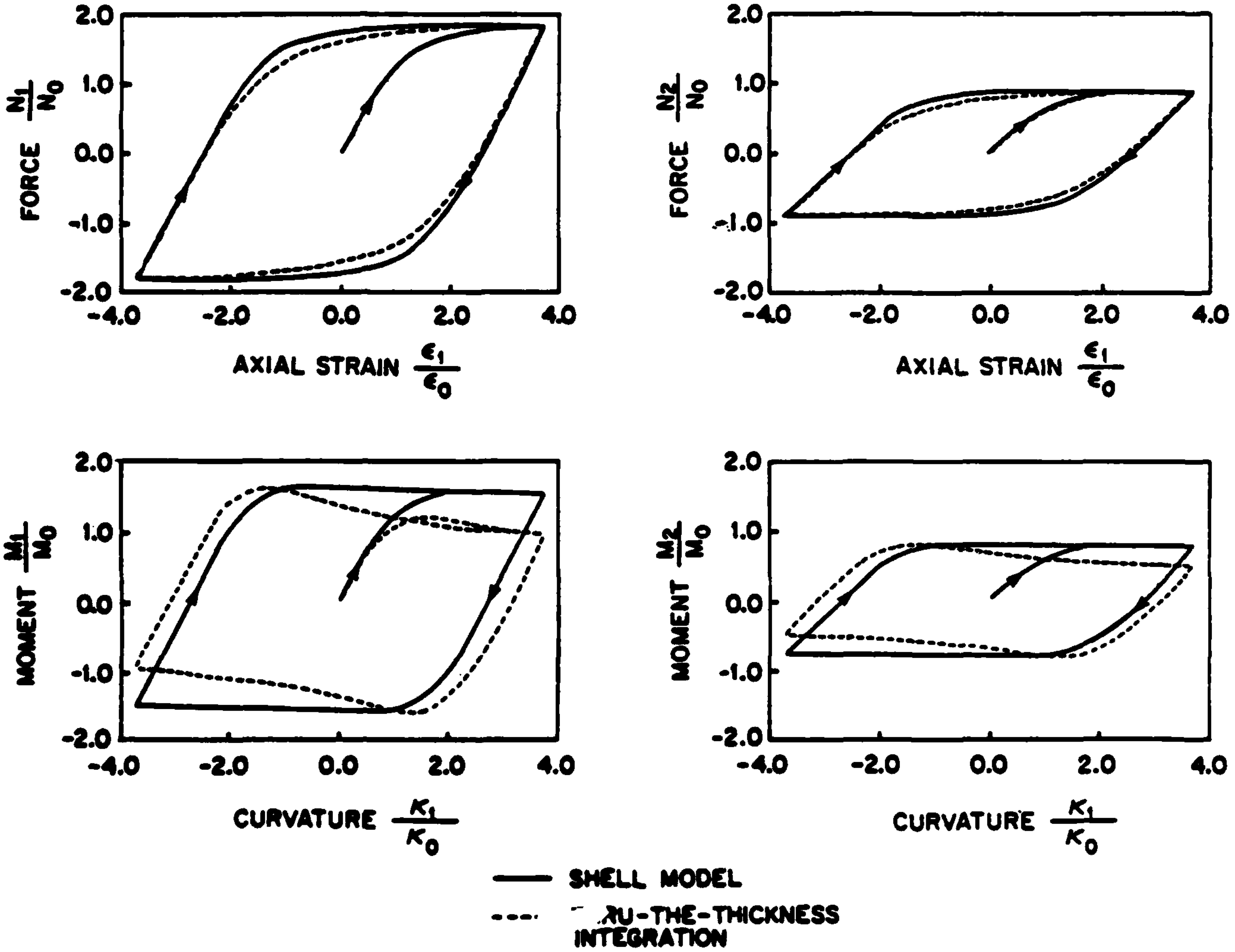

VISCOPLASTIC SHELL BEHAVIOR

LOADING RATE = 120 1/SEC

FIG. 12

LOADING CASE No. 5b

N_1	N_2	M_1	M_2
N	αN	M	βM

N_1, M_1 DOMINATE

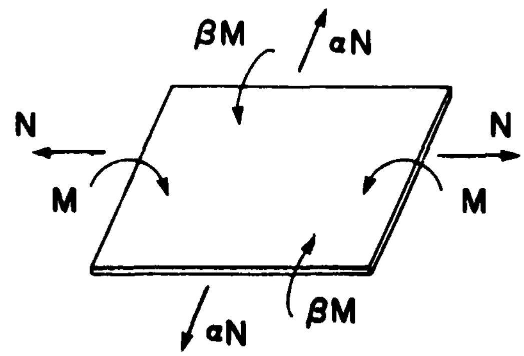

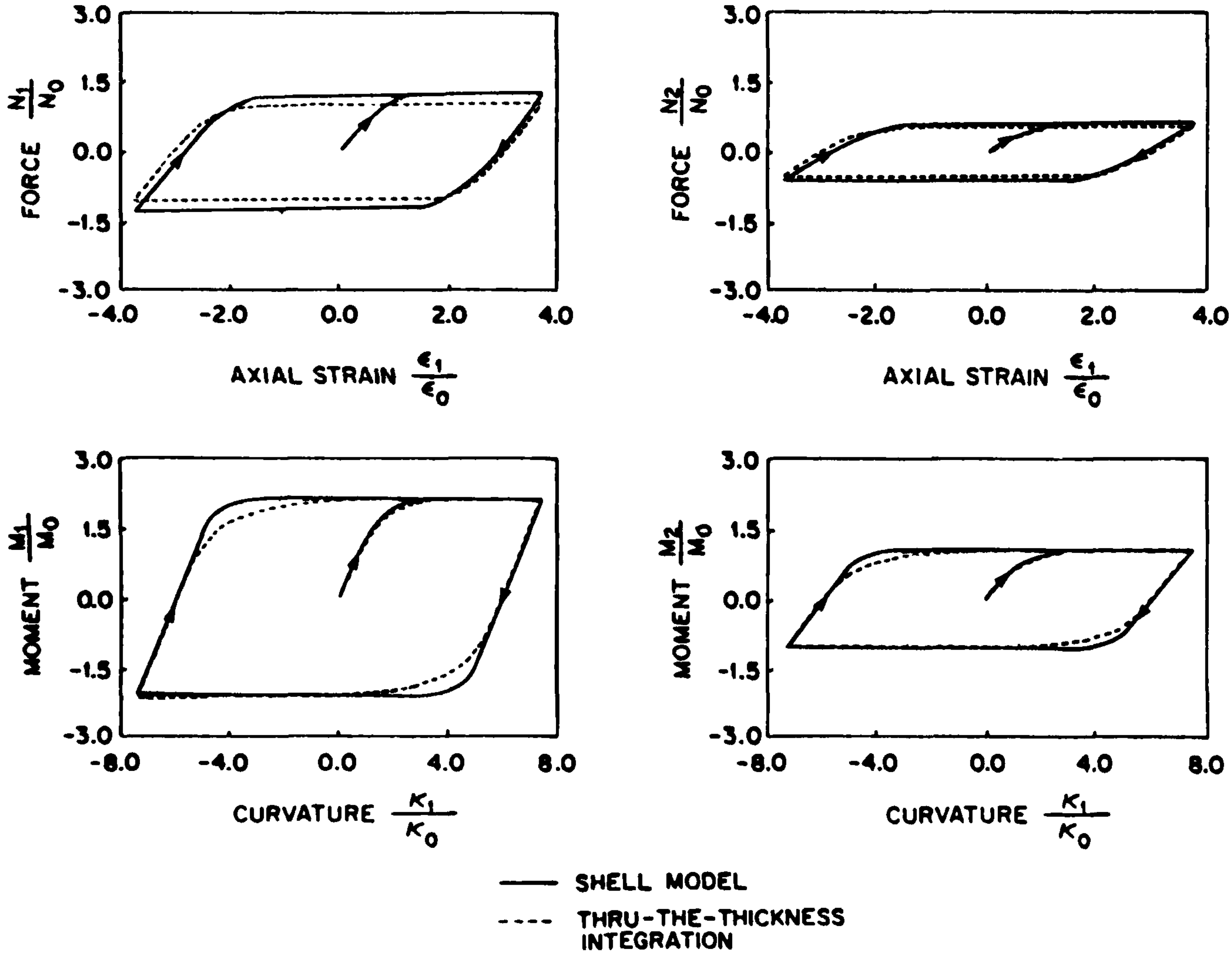

VISCOPLASTIC SHELL BEHAVIOR

LOADING RATE = 120 1/SEC

FIG. 13

LOADING CASE No. 6

N_1	N_2	M_1	M_2
N	αN	M	βM

N_1, M_2 DOMINATE

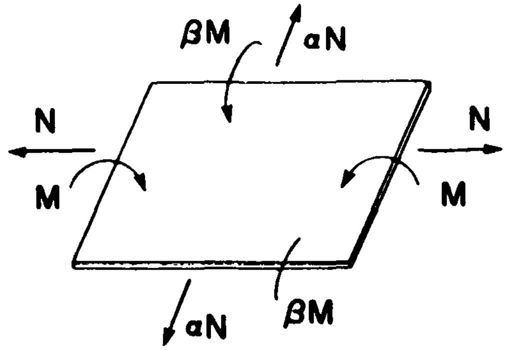

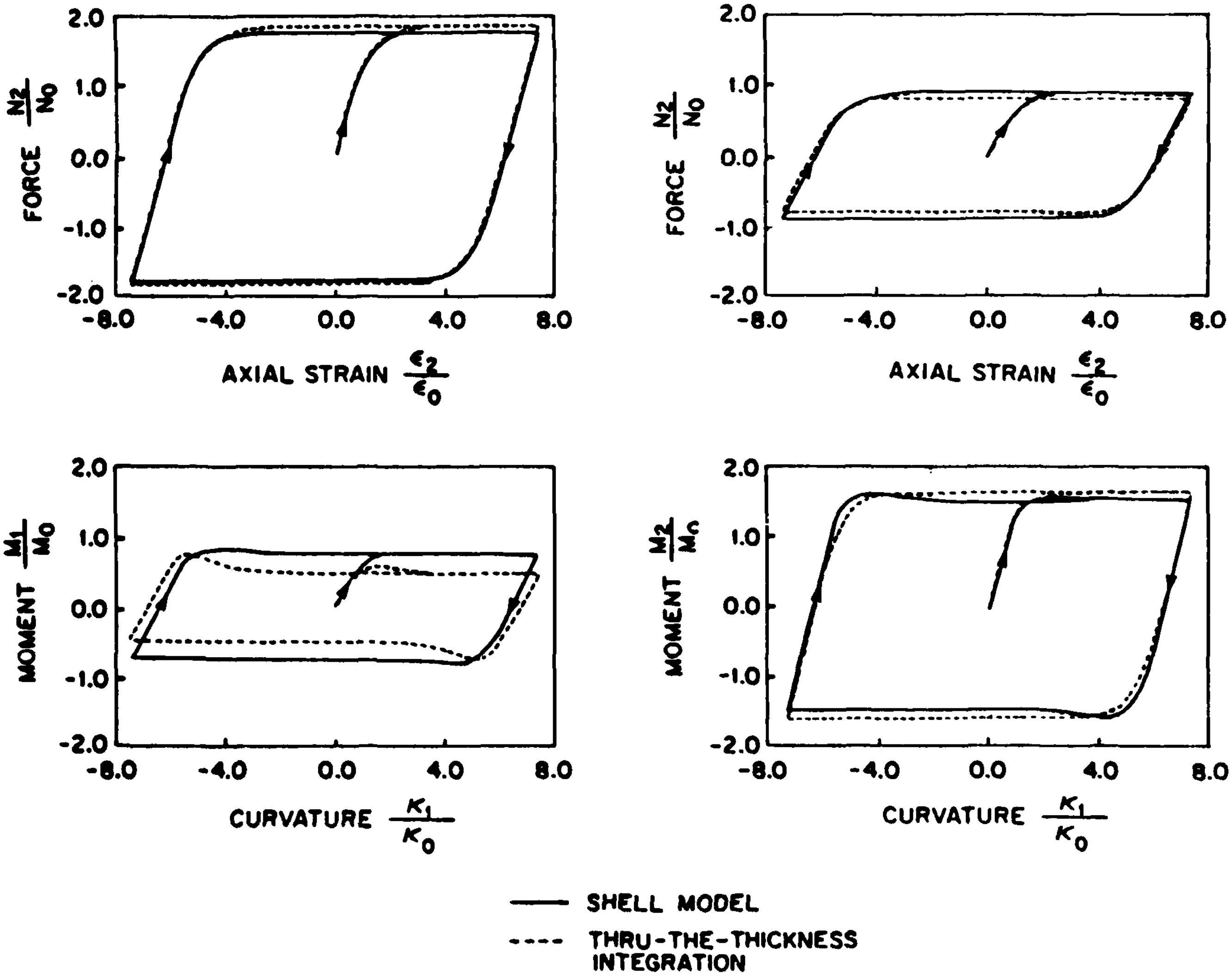

VISCOPLASTIC SHELL BEHAVIOR

LOADING RATE = 120 1/SEC

FIG.14

LOADING CASE No. 7a

N_1	N_2	M_1	M_2
N	N	M	M

BIAXIAL FORCE AND MOMENT

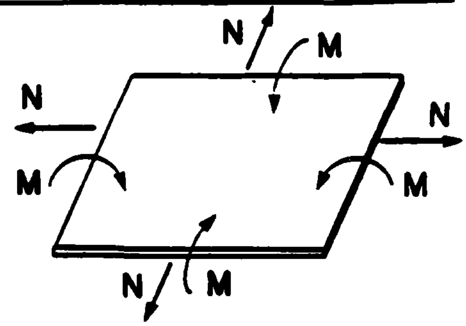

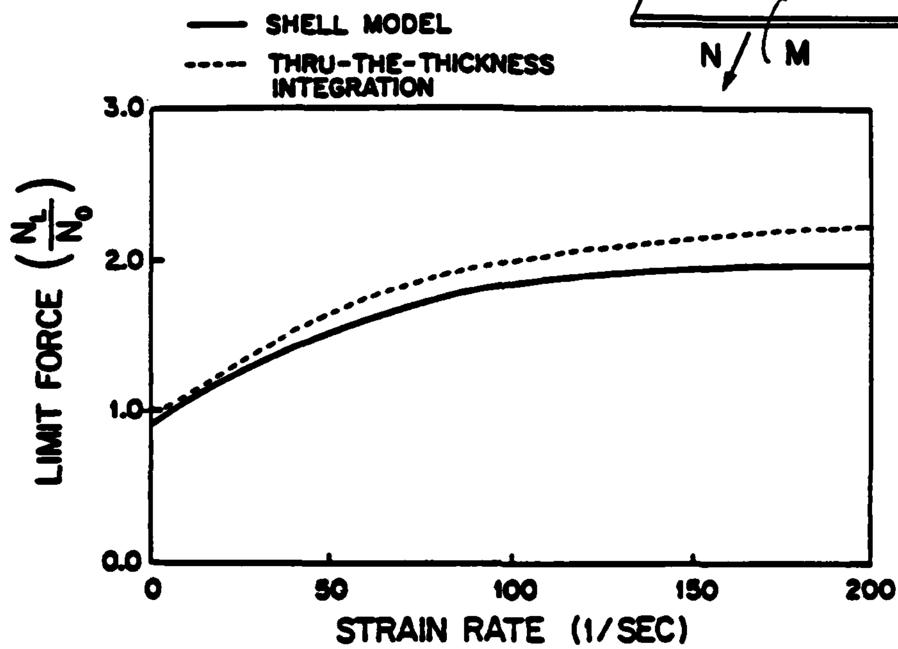

LIMIT FORCE VS. LOADING RATE

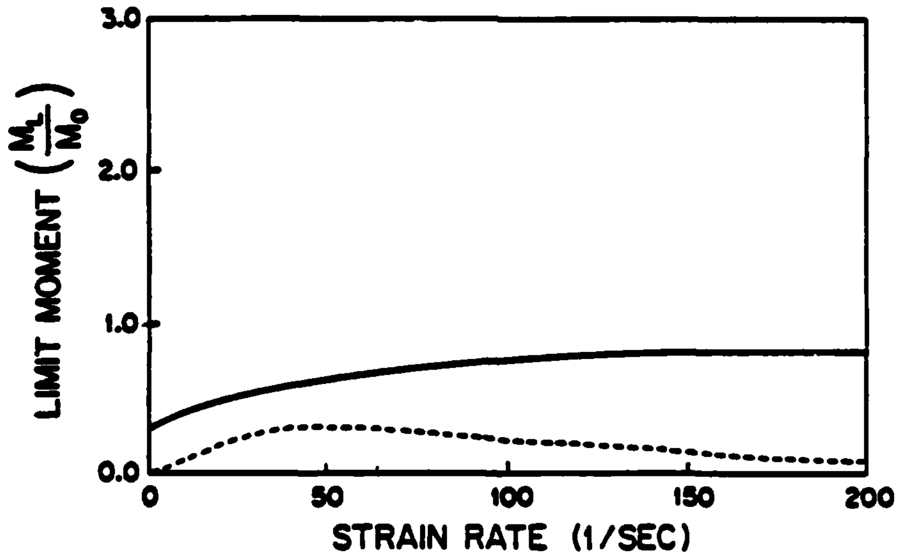

LIMIT MOMENT VS. LOADING RATE

VISCOPLASTIC SHELL BEHAVIOR

STRESS RESULTANT LIMITS VS. LOADING RATE

$$\frac{\Delta\kappa}{\Delta\epsilon} = 1.0$$

FIG. 15

LOADING CASE No. 7b

N_1	N_2	M_1	M_2
N	N	M	M

BIAXIAL FORCE AND MOMENT

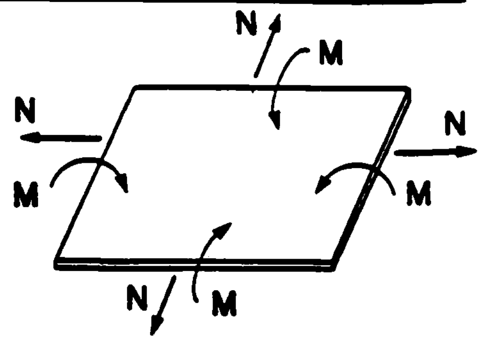

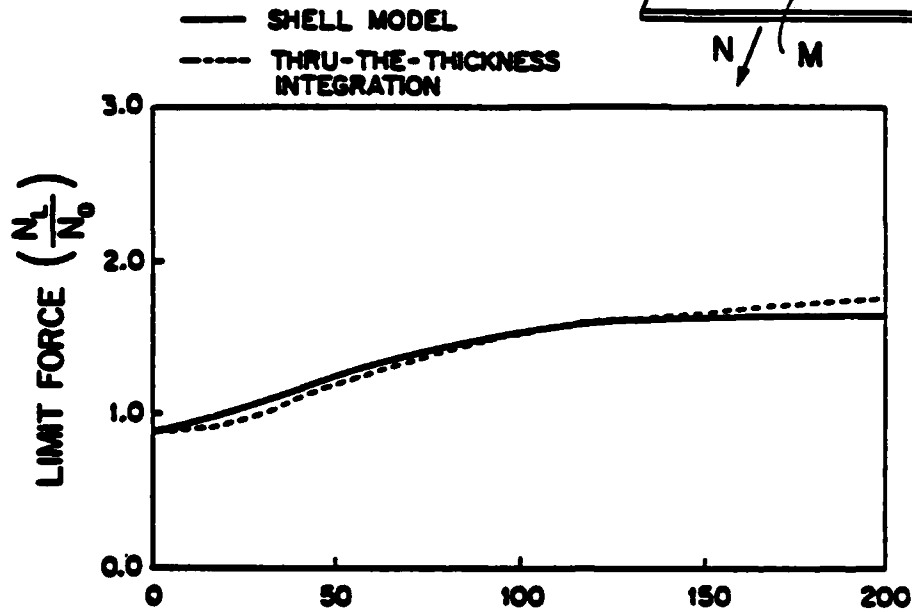

LIMIT FORCE VS. LOADING RATE

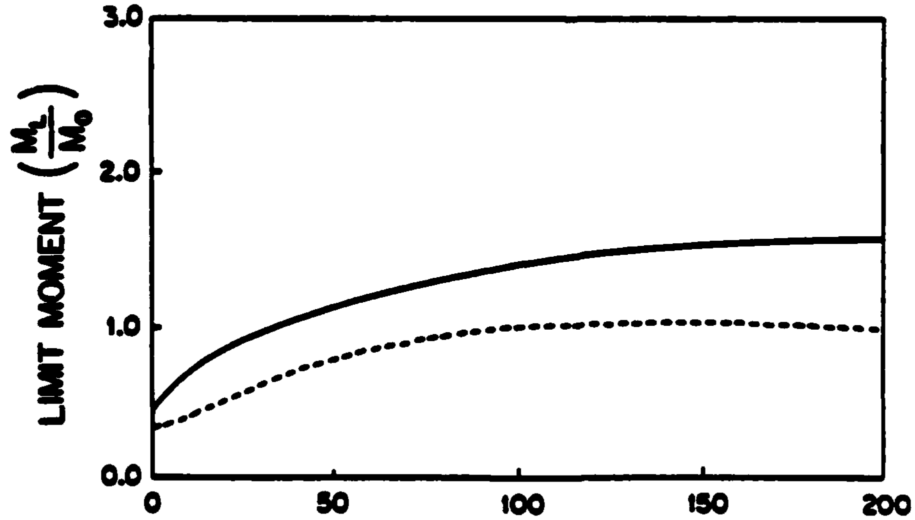

LIMIT MOMENT VS. LOADING RATE

VISCOPLASTIC SHELL BEHAVIOR

STRESS RESULTANT LIMITS VS. LOADING RATE

$$\frac{\Delta\kappa}{\Delta\epsilon} = 2.25$$

FIG. 16

LOADING CASE No. 7c

N_1	N_2	M_1	M_2
N	N	M	M

BIAXIAL FORCE AND MOMENT

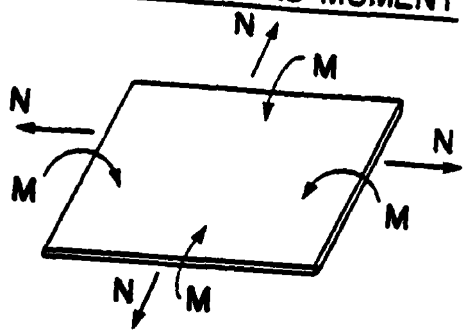

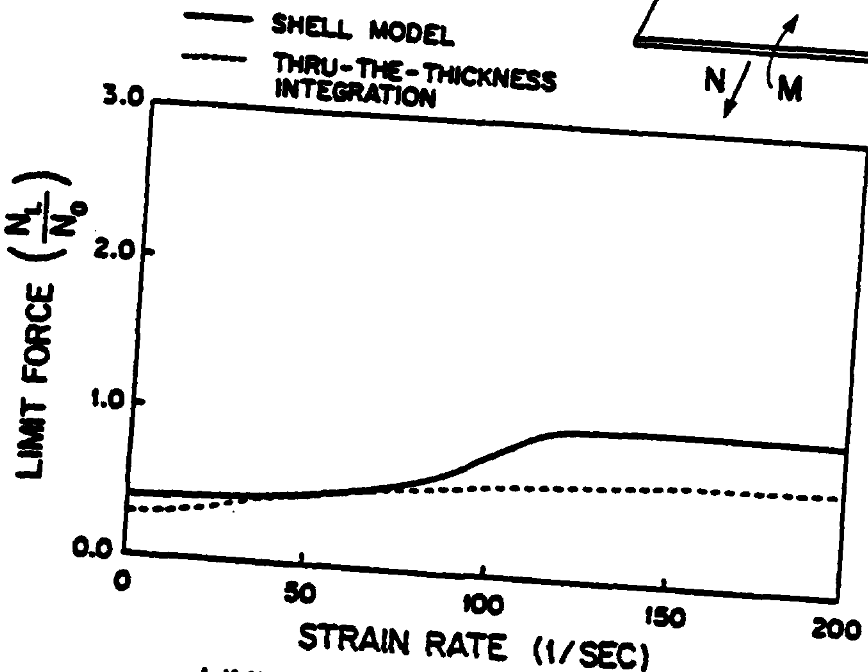

LIMIT FORCE VS. LOADING RATE

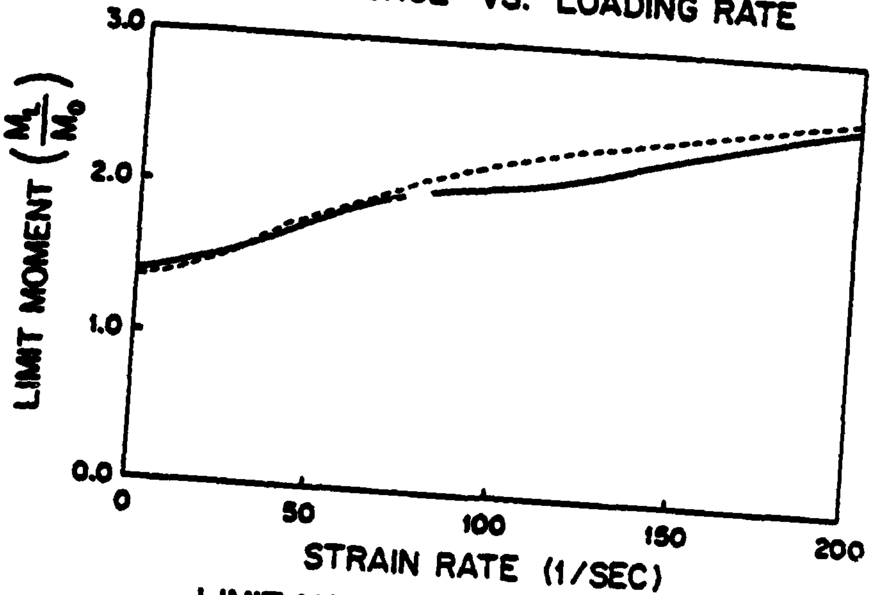

LIMIT MOMENT VS. LOADING RATE

VISCOPLASTIC SHELL BEHAVIOR

STRESS RESULTANT LIMITS VS. LOADING RATE

$$\frac{\Delta \kappa}{\Delta \epsilon} = 6.25$$

FIG. 17

LOADING CASE No. 7d

BIAXIAL FORCE AND MOMENT

N_1	N_2	M_1	M_2
N	N	M	M

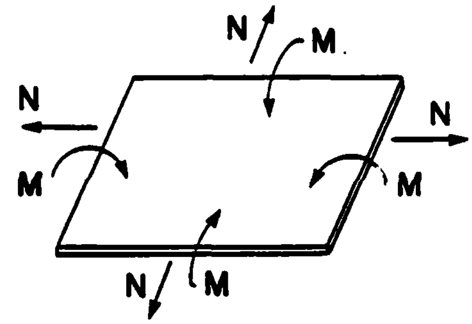

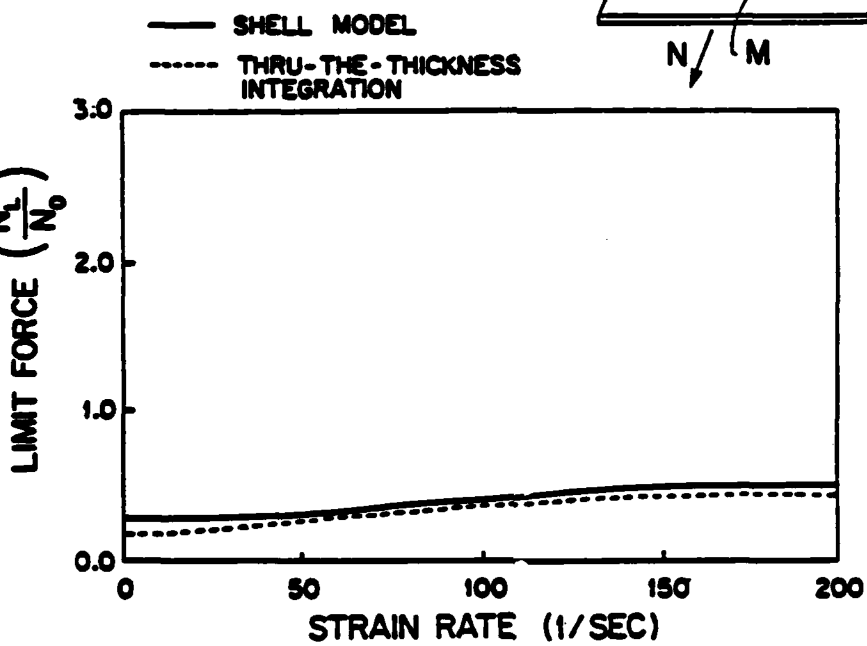

LIMIT FORCE VS. LOADING RATE

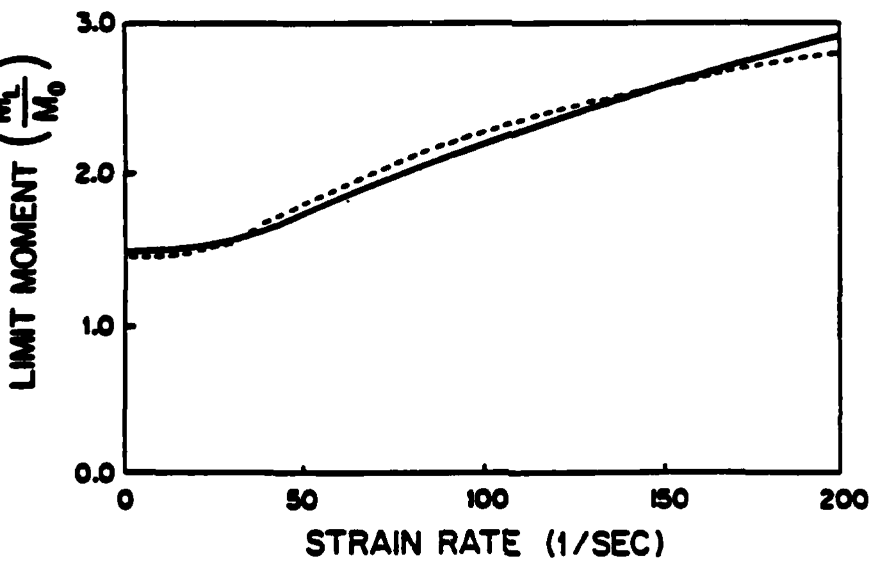

LIMIT MOMENT VS. LOADING RATE

VISCOPLASTIC SHELL BEHAVIOR

STRESS RESULTANT LIMITS VS. LOADING RATE

$$\frac{\Delta \kappa}{\Delta \epsilon} = 10.0$$

FIG. 18

LOADING CASE No. 8

BIAXIAL FORCE AND MOMENT

N_1	N_2	M_1	M_2
N	N	M	-M

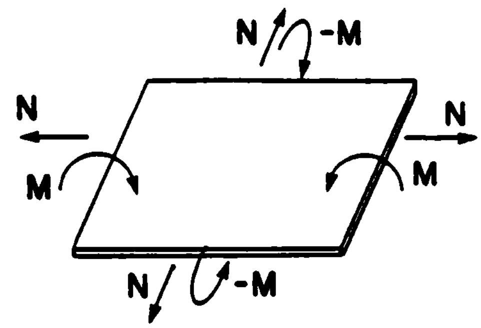

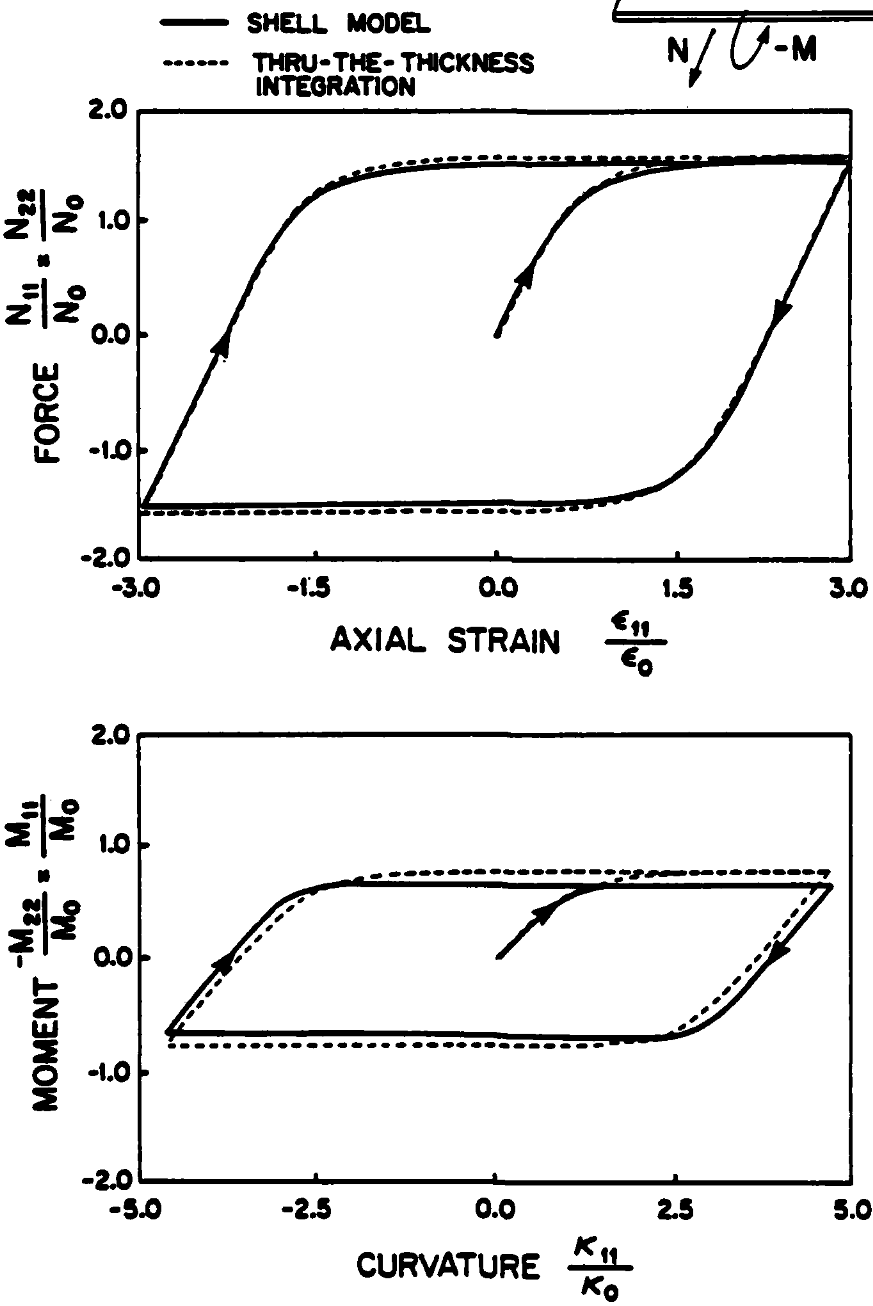

VISCOPLASTIC SHELL BEHAVIOR

LOADING RATE = 120 1/SEC

FIG. 19

LOADING CASE No. 9

BIAXIAL FORCE AND MOMENT

N_1	N_2	M_1	M_2
N	N	-M	-M

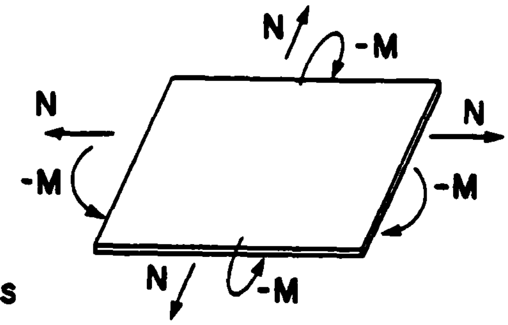

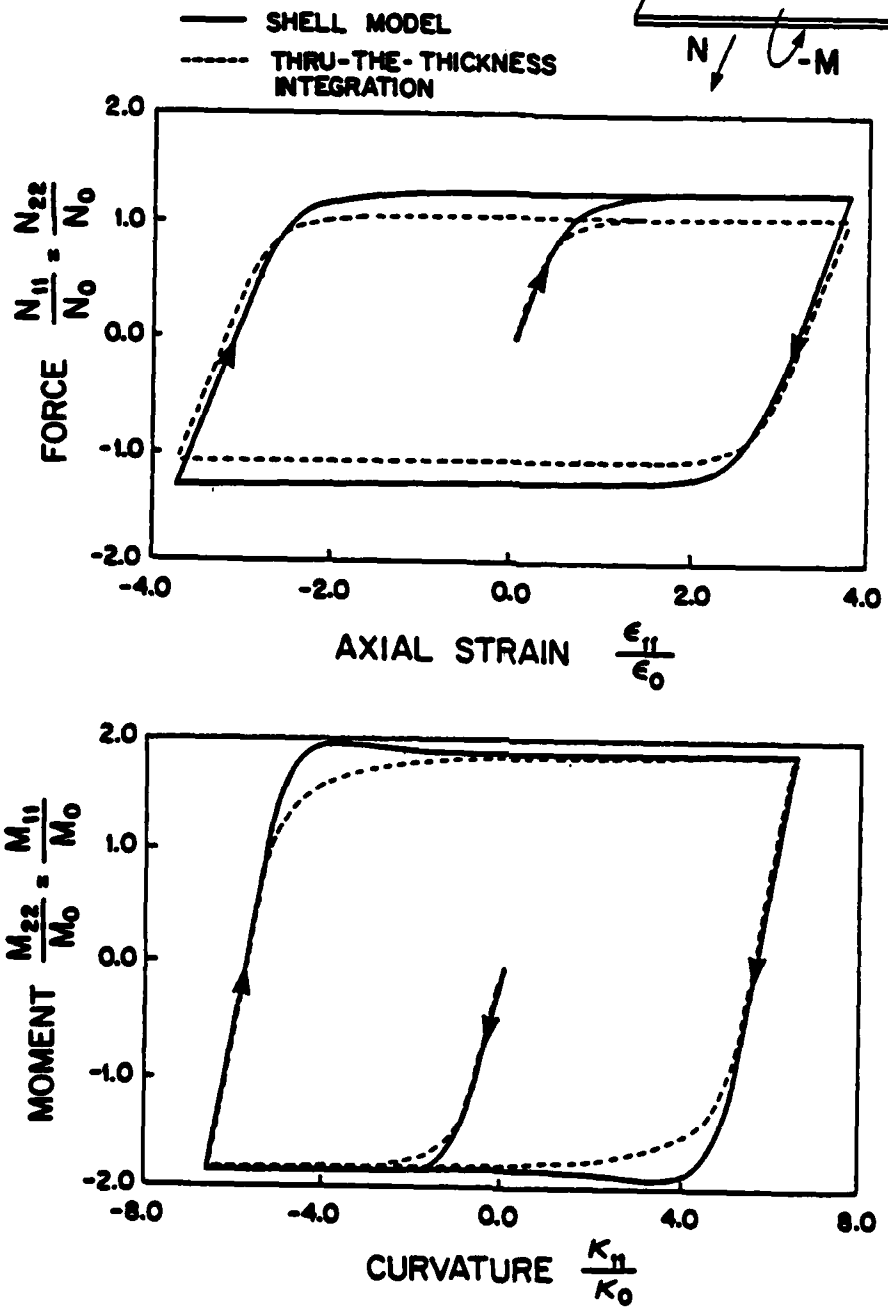

VISCOPLASTIC SHELL BEHAVIOR

LOADING RATE = 120 1/SEC

FIG. 20

LOADING CASE No. 10 — BIAXIAL FORCE AND MOMENT

N_1	N_2	M_1	M_2
N	-N	M	M

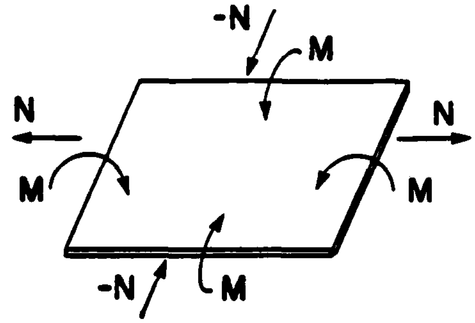

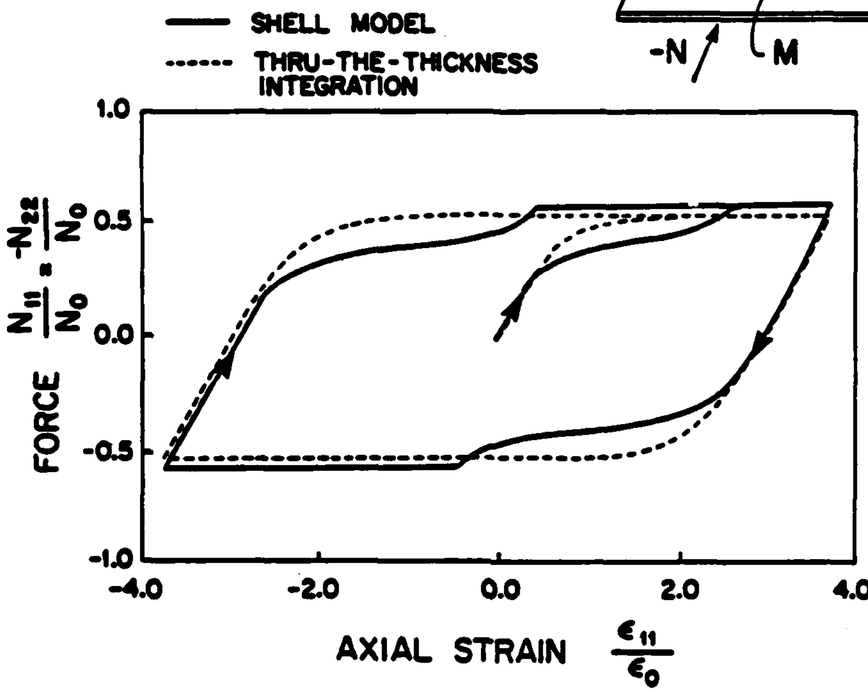

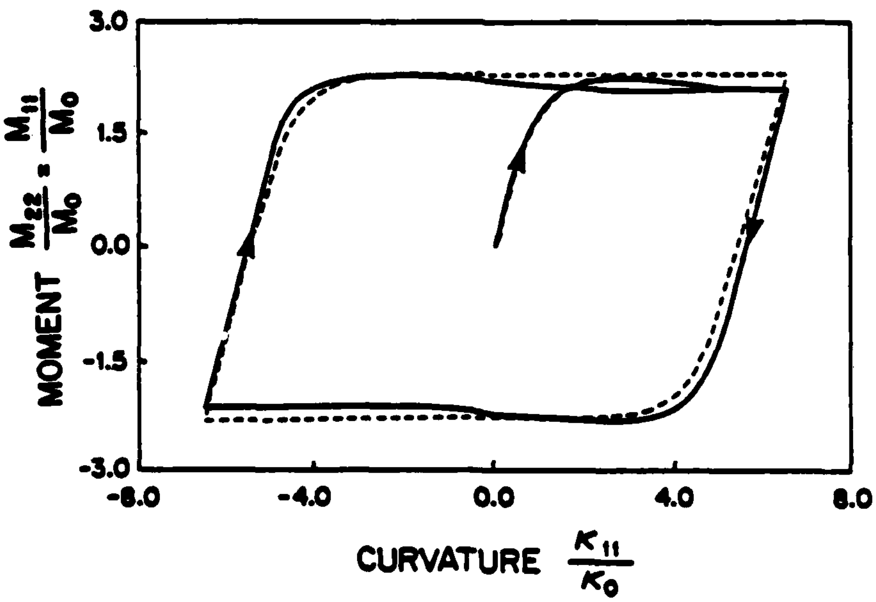

VISCOPLASTIC SHELL BEHAVIOR

LOADING RATE = 120 1/SEC

FIG. 21

LOADING CASE No. 11 BIAXIAL FORCE AND MOMENT

N_1	N_2	M_1	M_2
-N	N	-M	M

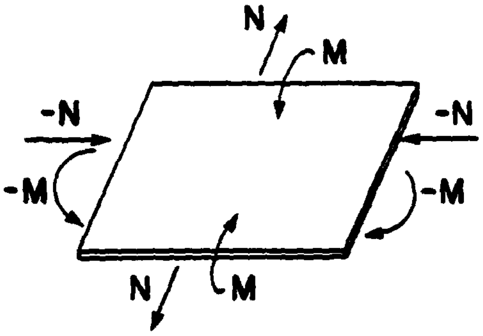

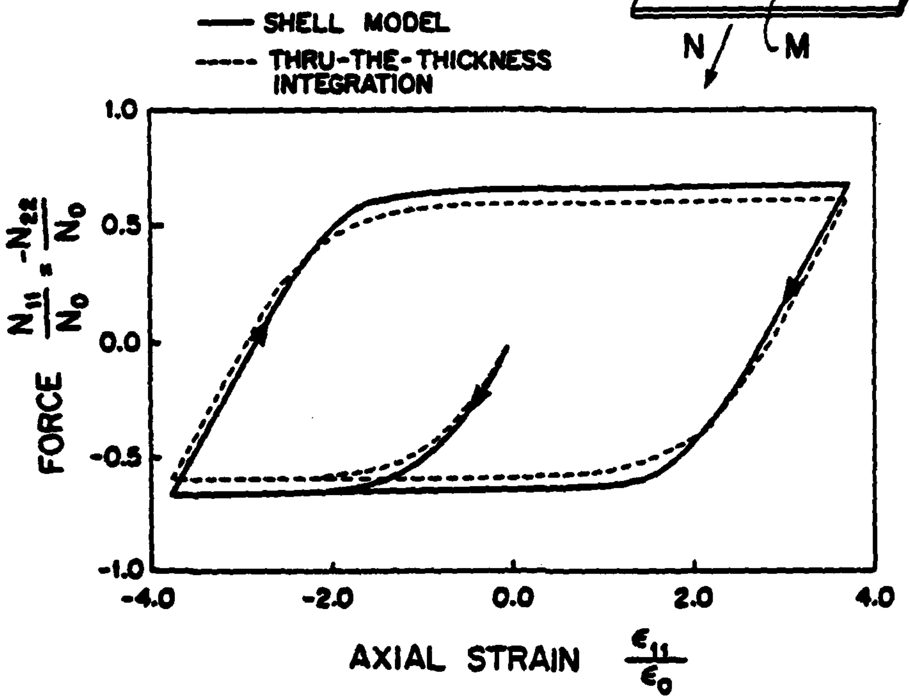

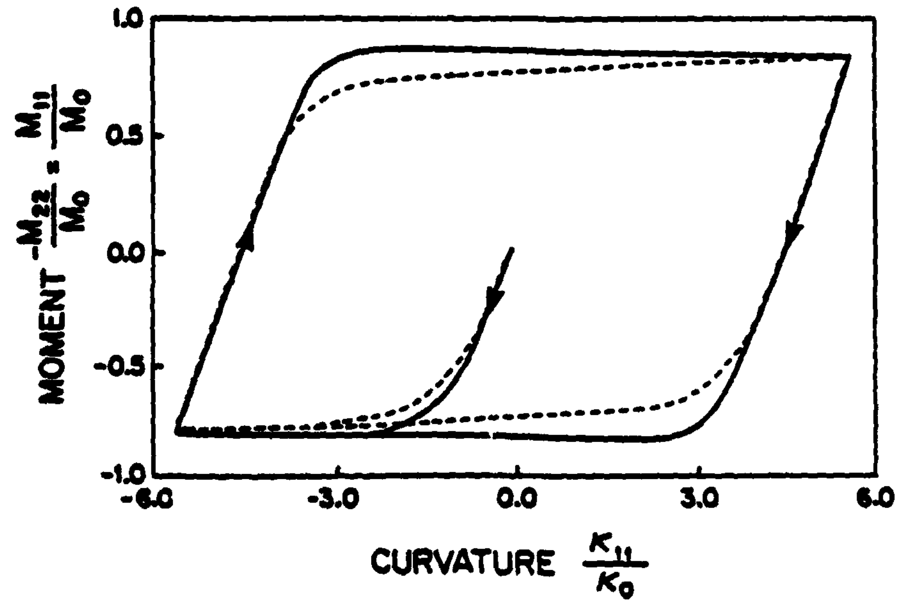

VISCOPLASTIC SHELL BEHAVIOR

LOADING RATE = 120 1/SEC

FIG. 22

LOADING CASE No. 12

BIAXIAL FORCE AND MOMENT

N_1	N_2	M_1	M_2
N	-N	-M	M

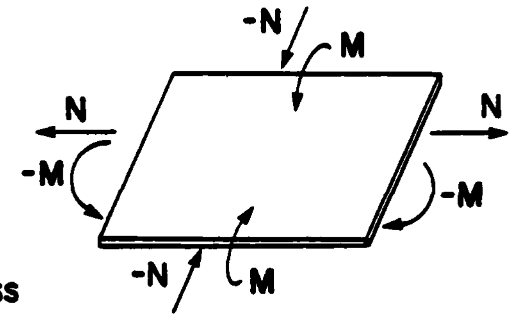

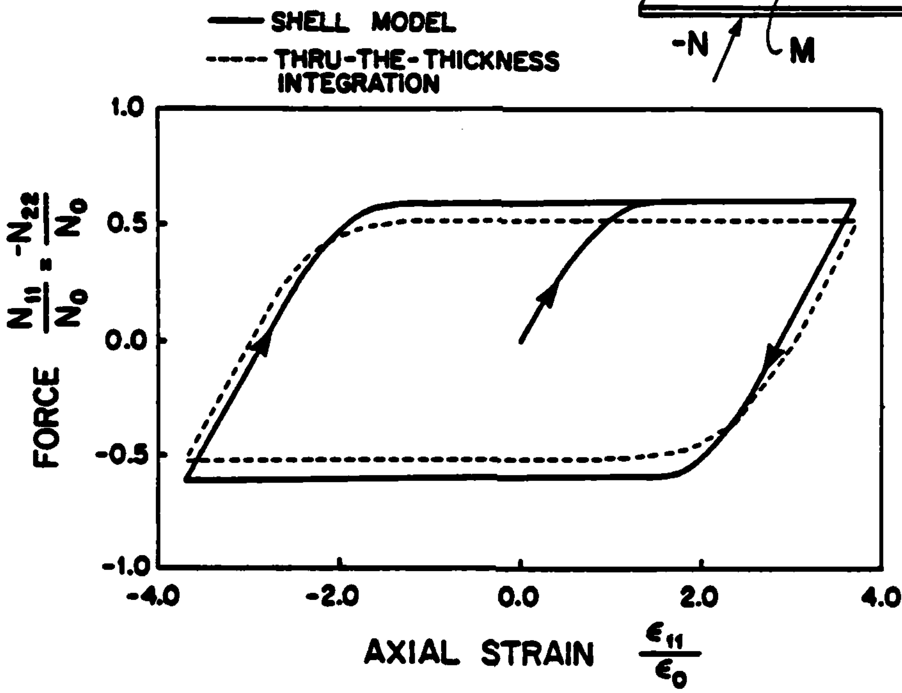

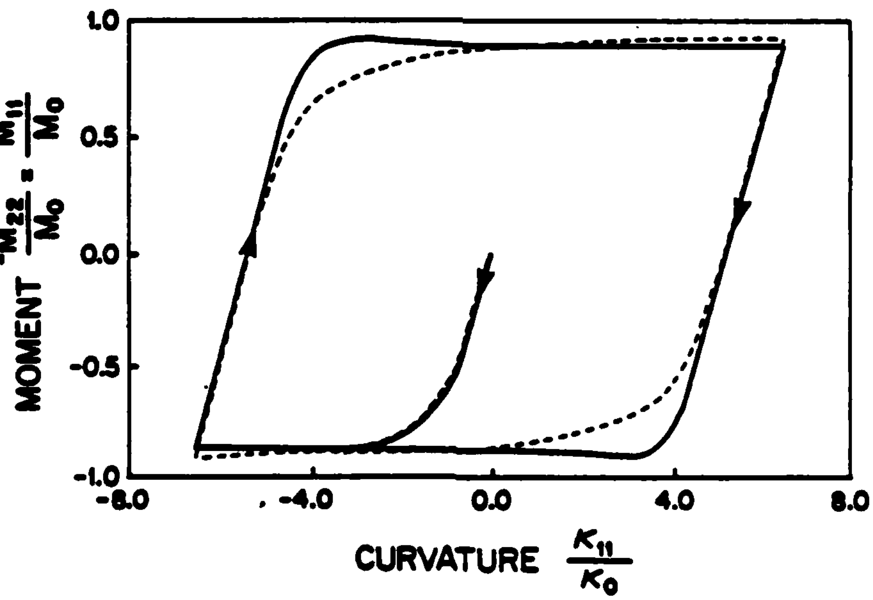

VISCOPLASTIC SHELL BEHAVIOR

LOADING RATE = 120 1/SEC

FIG. 23

NON-LINEAR TRANSIENT RESPONSE OF CYLINDRICAL PANEL

STUDY OF VISCO-PLASTIC EFFECTS

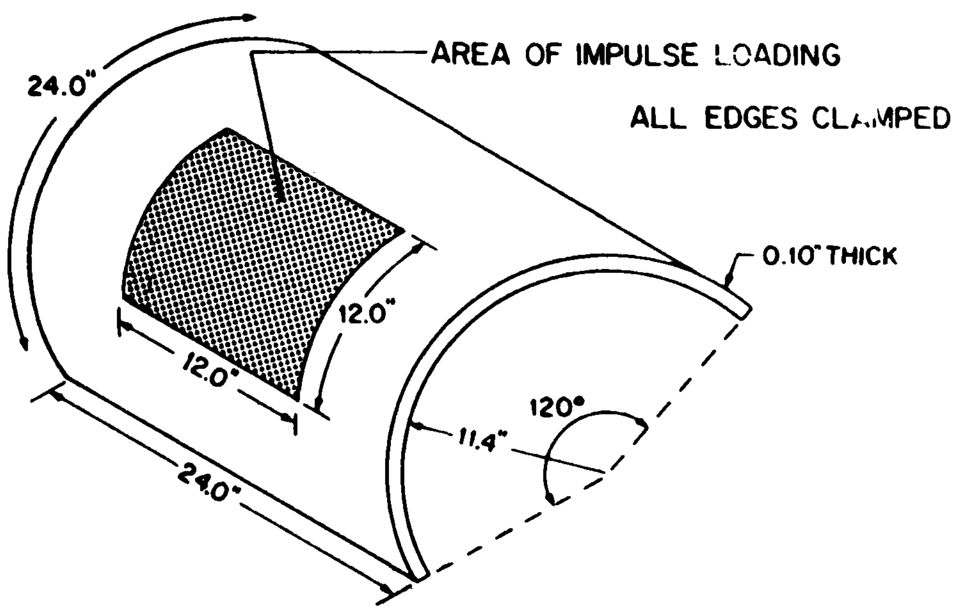

MATERIAL PROPERTIES

DENSITY:	7.33×10^{-4} LB-SEC^2/ IN^4
CURVATURE:	0.0877
YOUNG'S MODULUS:	30×10^6 PSI
POISSON'S RATIO:	0.3
STATIC YIELD STRENGTH:	40,000 PSI

FIG. 24

EPSA FINITE ELEMENT MODEL (1/4 PANEL)

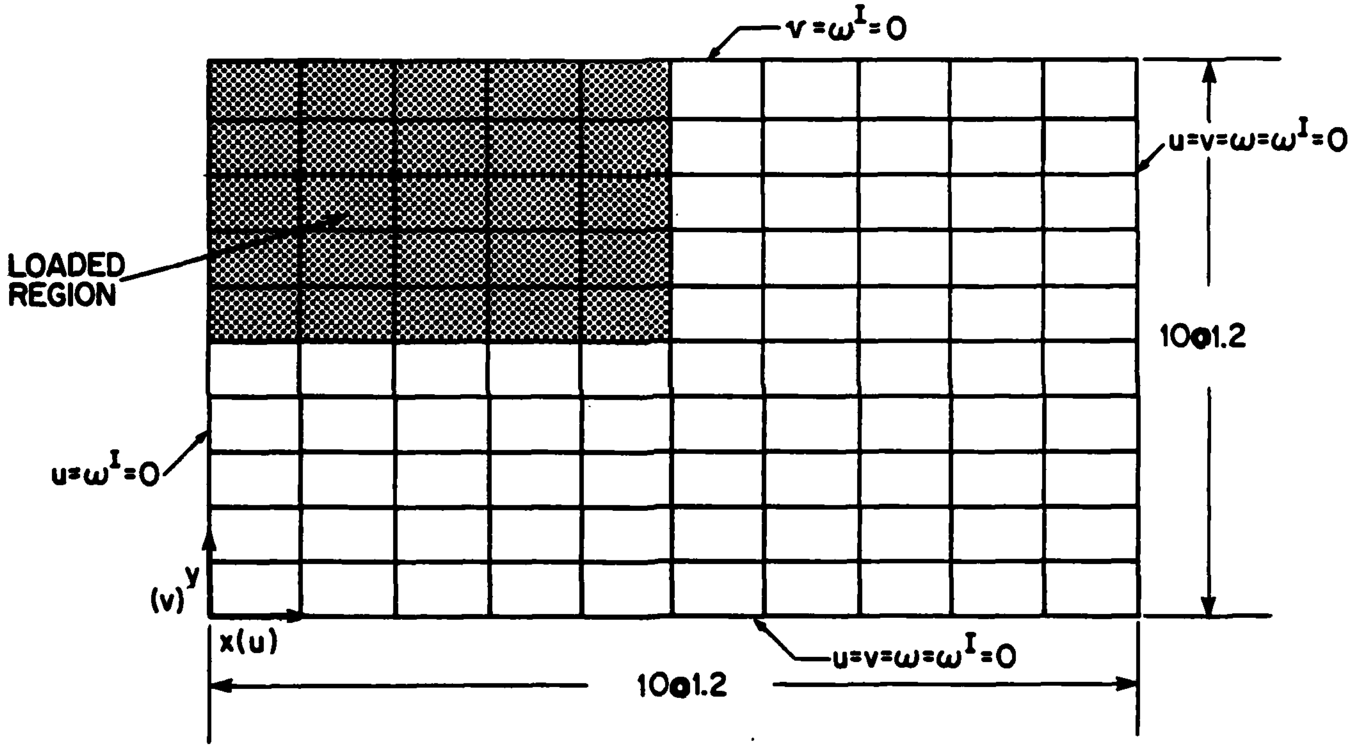

INITIAL NORMAL VELOCITIES SPECIFIED FOR LOADED REGION

$\dot{q}_z = 2250$ in/sec

FIG. 25

NON-LINEAR VISCOPLASTIC RESPONSE OF CYLINDRICAL PANEL SUBJECTED TO TRANSIENT LOADING

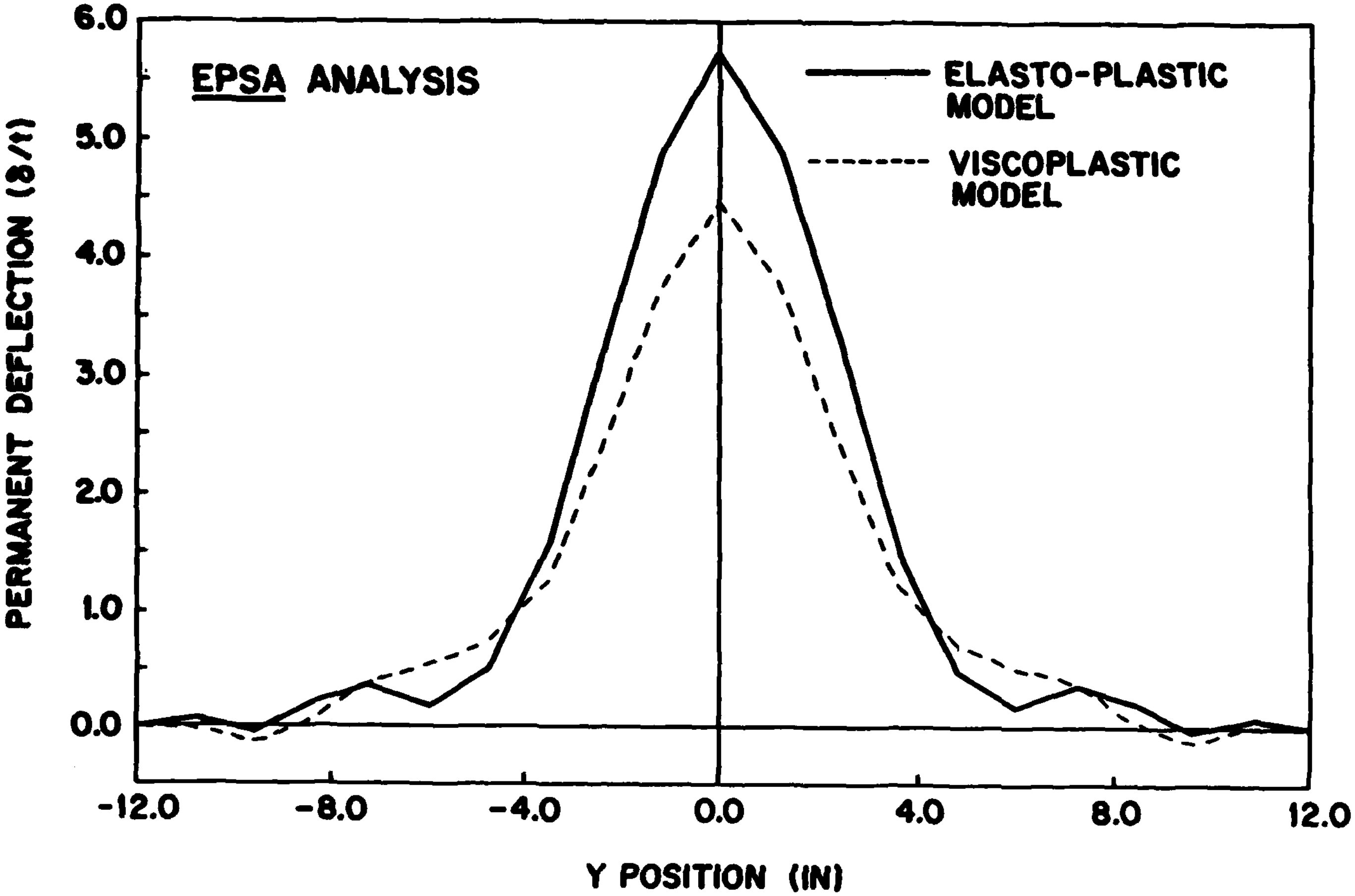

PERMANENT DEFLECTION ALONG CENTERLINE OF STRUCTURE

FIG. 26

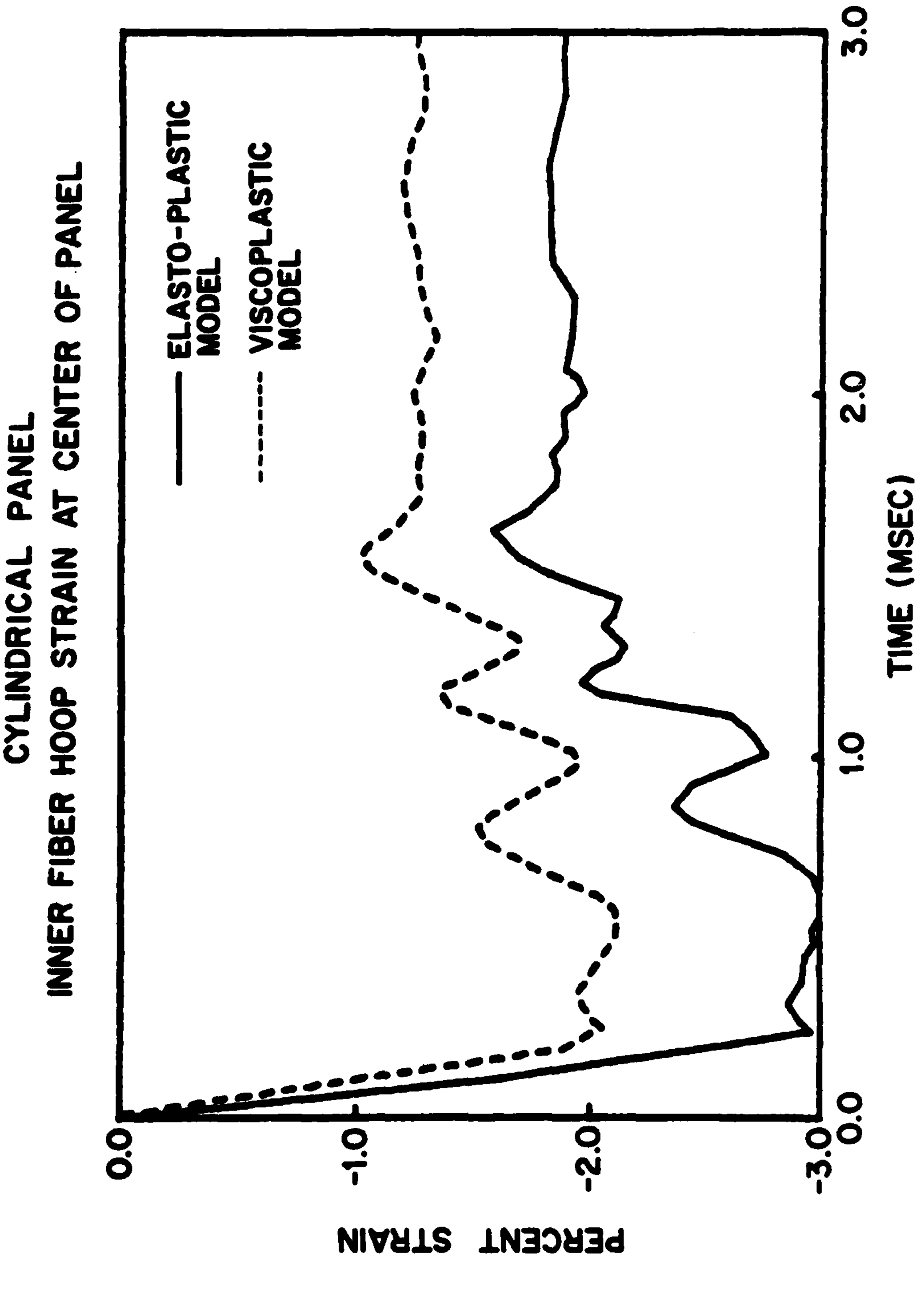

CYLINDRICAL PANEL
INNER FIBER HOOP STRAIN AT CENTER OF PANEL
ELASTO-PLASTIC MODEL
VISCOPLASTIC MODEL
PERCENT STRAIN
0.0
-1.0
-2.0
-3.0
TIME (MSEC)
0.0
1.0
2.0
3.0

FIG. 27

STIFFENED CYLINDRICAL SHELL
IMMERSED IN AN ACOUSTIC MEDIUM

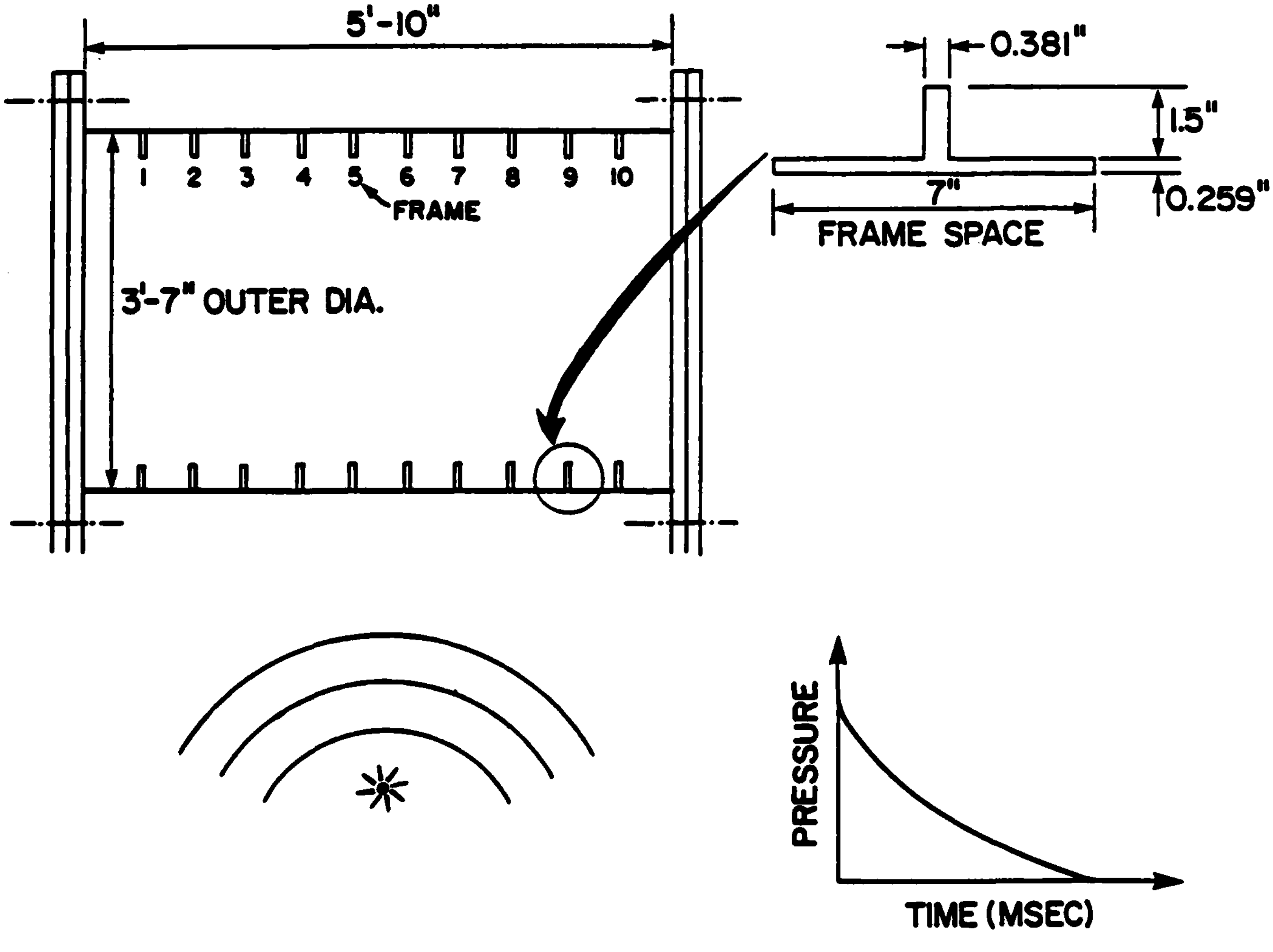

FIG. 28

PERMANENT DEFLECTION
OF
STIFFENED CYLINDRICAL SHELL
SUBJECTED TO
DYNAMIC LOADING

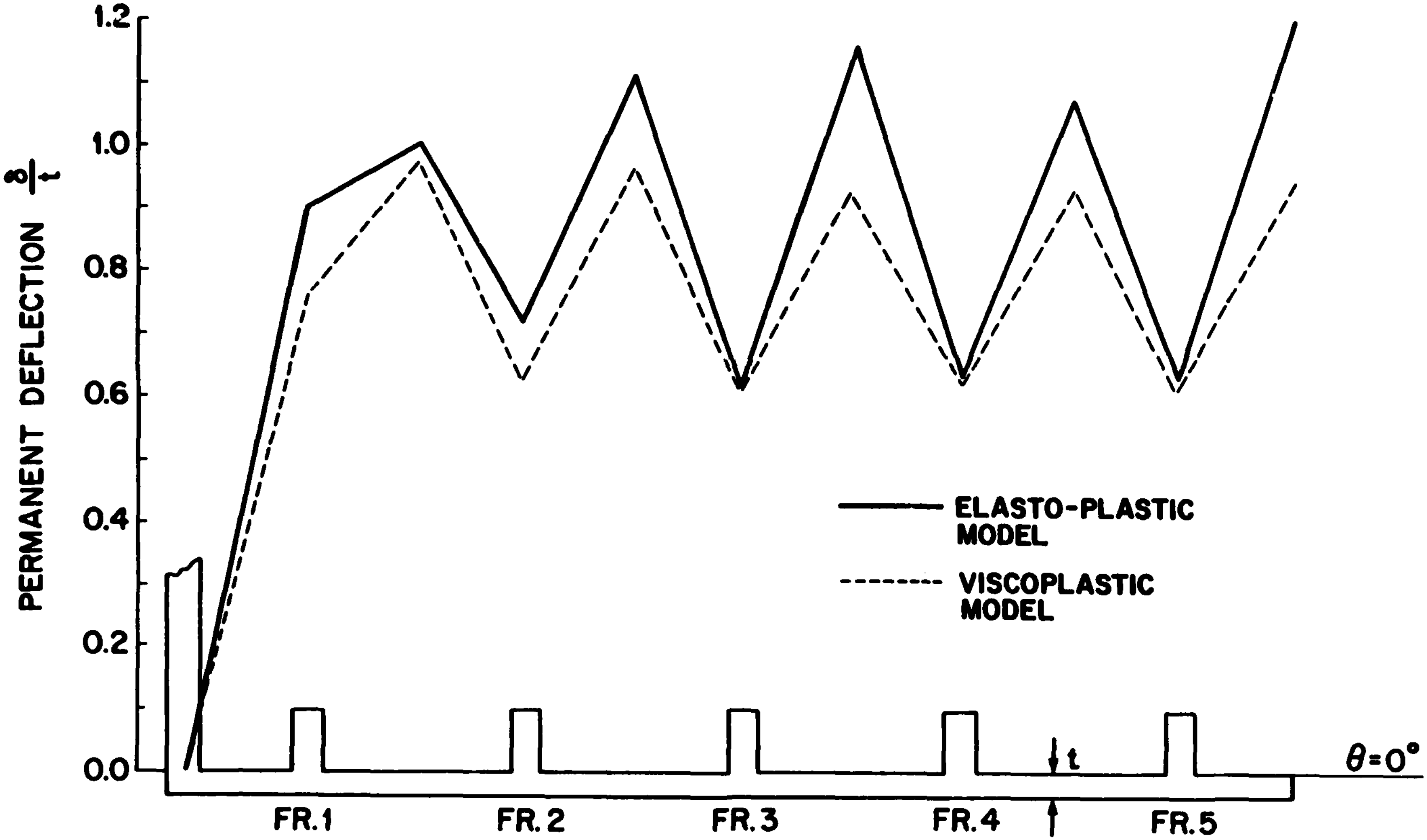

FIG. 29

STIFFENED CYLINDRICAL SHELL

EPSA ANALYSIS

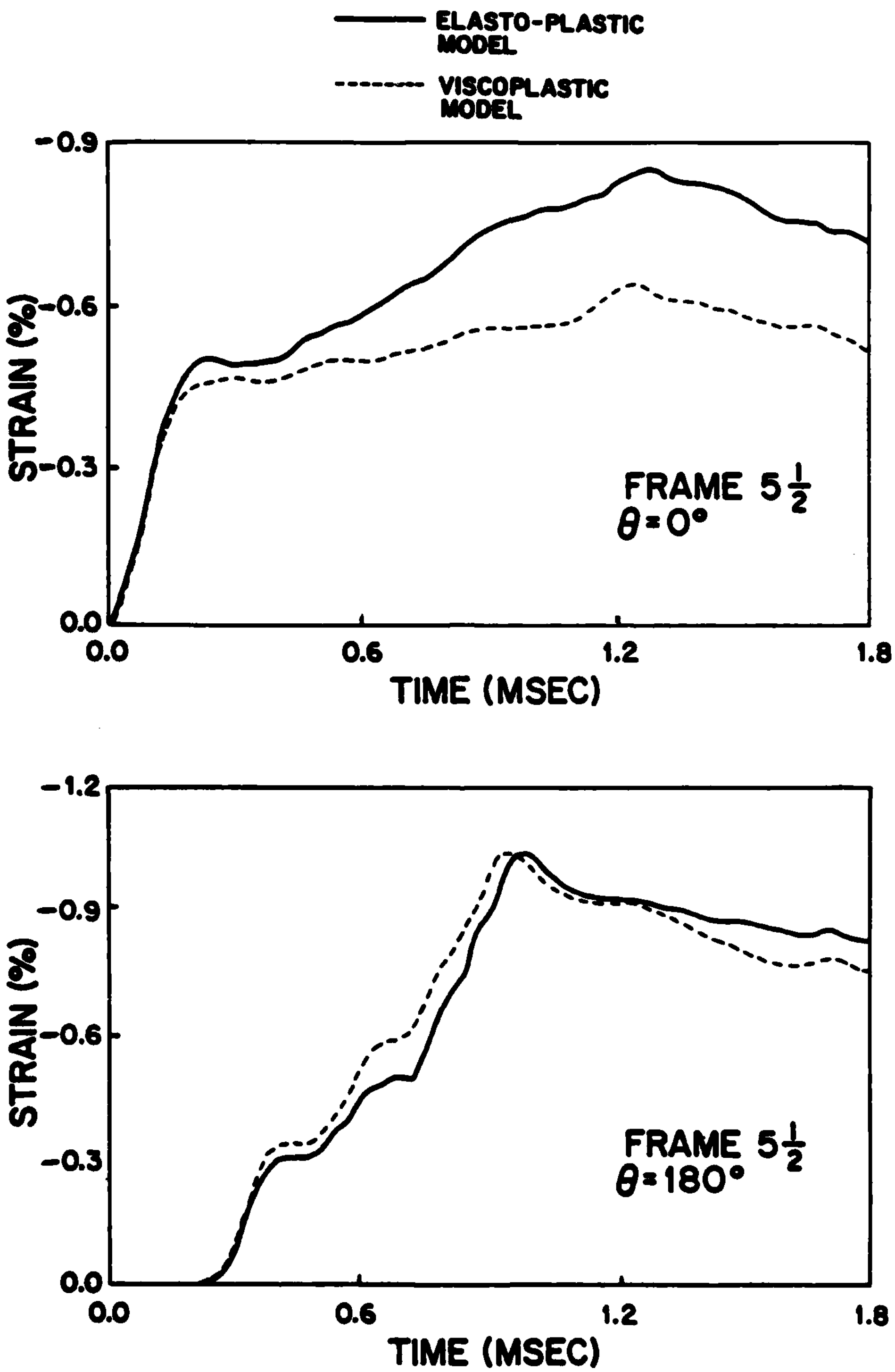

INNER FIBER HOOP STRAIN

FIG. 30

DISTRIBUTION LIST

DEPARTMENT OF DEFENSE

Assistant to the Secretary of Defense
Atomic Energy
ATTN: Exec Asst

Defense Advanced Rsch Proj Agency
ATTN: TIO

Defense Intelligence Agency
ATTN: DB-4C2
ATTN: DB-4C2, C. Wiehle
ATTN: DT-1C
ATTN: DT-2
ATTN: RTS-2A
ATTN: DB-4C3
ATTN: DB-4C, Rsch, Phys Vuln Br
ATTN: DB-4C1

Defense Nuclear Agency
ATTN: SPSS
ATTN: STSP
4 cy ATTN: TITL

Defense Technical Information Ctr
12 cy ATTN: DD

Field Command Defense Nuclear Agency
Det 1
Lawrence Livermore Lab
ATTN: FC-1

Field Command
Defense Nuclear Agency
ATTN: FCPR
ATTN: FCT
ATTN: FCTX
ATTN: FCTT, G. Ganong
ATTN: FCTT, W. Summa
ATTN: FCTXE

Field Command Test Directorate
ATTN: FCTC

Interservice Nuclear Weapons School
ATTN: TTV

Joint Strat Tgt Planning Staff
ATTN: NRI-STINFO Library
ATTN: JLA, Threat Appl Div
ATTN: JLTW, R. Autenberg
ATTN: JLTW-2
ATTN: DOXT
ATTN: XPFS

Under Secretary of Defense for Rsch & Engrg
ATTN: Strat & Space Sys (OS)

DEPARTMENT OF THE ARMY

BMD Advanced Technology Ctr
ATTN: ICRDABH-X
ATTN: ATC-T

Chief of Engineers
ATTN: DAEN-RDL
ATTN: DAEN-MPE-T

DEPARTMENT OF THE ARMY (Continued)

Deputy Chief of Staff for Ops & Plans
ATTN: DAMO-NC, Nuc Chem Dir

Deputy Chief of Staff for Rsch Dev & Acq
ATTN: DAMA

Engineer Studies Ctr
ATTN: DAEN-FES, LTC Hatch

Harry Diamond Labs
ATTN: DELHD-NW-P, 20240
ATTN: DELHD-TA-L, 81100

USA Concepts Analysis Agency
ATTN: CSSA-ADL

USA Engineer Ctr & Ft Belvoir
ATTN: ATZA-DTE-ADM

USA Engineer School
ATTN: ATZA-CDC

USA Engr Waterways Exper Station
ATTN: R. Whalin
ATTN: WESSE
ATTN: WESSD, J. Jackson
ATTN: J. Strange
ATTN: J. Zelasko
ATTN: F. Brown
ATTN: Library
ATTN: WESSA, W. Flathau
ATTN: WESSS, J. Ballard

USA Foreign Science & Tech Ctr
ATTN: DRXST-SD

USA Mat Cmd Proj Mgr for Nuc Munitions
ATTN: DRCPM-NUC

USA Material & Mechanics Rsch Ctr
ATTN: DRXMR, J. Mescall
ATTN: Tech Library

USA Materiel Dev & Readiness Cmd
ATTN: DRCDE-D, L. Flynn
ATTN: DRXAM-TL

USA Nuclear & Chemical Agency
ATTN: Library

USA War College
ATTN: Library

USA Military Academy
ATTN: Doc Library

USA Missile Cmd
ATTN: Doc Sec
ATTN: DRSMI-RH

DEPARTMENT OF THE NAVY

Marine Corp Dev & Ed Cmd
ATTN: D091, J. Hartneady

DEPARTMENT OF THE NAVY (Continued)

David Taylor Naval Ship R&D Ctr
ATTN: Code L42-3
ATTN: Code 1700, W. Murray
ATTN: Code 1844
ATTN: Code 177, E. Palmer
ATTN: Code 172
ATTN: Code 1770.1
ATTN: Code 174
ATTN: Code 2740
ATTN: Code 1740.4
ATTN: Code 1740, R. Short
ATTN: Code 173
ATTN: Code 1!
ATTN: Code 1740.5
ATTN: Code 1740.6
ATTN: Code 1740.1

Marine Corps
ATTN: POM

Naval Civil Engineering Lab
ATTN: Code L51, J. Crawford

Naval Coastal Systems Lab
ATTN: Code 741

Naval Electronic Systems Cmd
ATTN: PME 117-21

Naval Explosive Ord Disposal Fac
ATTN: Code 504, J. Petrousky

Naval Facilities Engineering Cmd
ATTN: Code 04B

Naval Material Cmd
ATTN: MAT 08T-22

Naval Ocean Systems Ctr
ATTN: Code 013, E. Cooper
ATTN: Code 4471

Naval Postgraduate School
ATTN: Code 69NE
ATTN: Code 1424, Library
ATTN: Code 69SG, Y Shin

Naval Research Lab
ATTN: Code 8403, R. Belsham
ATTN: Code 8440, G. O'Hara
ATTN: Code 6380
ATTN: Code 8100
ATTN: Code 8301
ATTN: Code 8406
ATTN: Code 2627
ATTN: Code 8445
ATTN: Code 8404, H. Pusey

Naval Sea Systems Cmd
ATTN: SEA-033
ATTN: SEA-323
ATTN: SEA-06J, R Lane
ATTN: SEA-09G53
ATTN: SEA-55X1
ATTN: SEA-08
ATTN: SEA-0351
ATTN: SEA-9931G

DEPARTMENT OF THE NAVY (Continued)

Naval Surface Wpns Ctr
ATTN: Code F34
ATTN: Code R13
ATTN: Code R10
ATTN: Code U401, M. Kleinerman
ATTN: Code R14
ATTN: Code F31
ATTN: Code R14
ATTN: Code R15

Naval Surface Weapons Ctr
ATTN: W. Wishard
ATTN: Tech Library & Info Svcs Br

Naval War College
ATTN: Code E-11, Tech Svc

Naval Wpns Ctr
ATTN: Code 233
ATTN: Code 266, C. Austin
ATTN: Code 3263, J. Bowen

Naval Weapons Evaluation Facility
ATTN: G. Binns
ATTN: Code 10
ATTN: Code 210
ATTN: R. Hughes

Naval Weapons Support Ctr
ATTN: Code 70553, D. Moore

New London Lab
Naval Underwater Systems Ctr
ATTN: Code 4494, J. Patel
ATTN: Code 4492, J. Kalinowski

Newport Lab
Naval Underwater Systems Ctr
ATTN: Code EM
ATTN: Code 363, P. Paranzino

Office of the Deputy Chief of Naval Ops
ATTN: OP 987
ATTN: NOP 982, Tac Air Srf & EWDEV Div
ATTN: NOP 981
ATTN: NOP 654, Strat Eval & Anal Br
ATTN: OP 098T8
ATTN: OP 982E, M. Lenzini
ATTN: OP 957E
ATTN: NOP 953, TAC Readiness Div
ATTN: OP 37
ATTN: OP 225
ATTN: OP 03EG
ATTN: OP 21
ATTN: NOP 951, ASW Div
ATTN: OP 605D5
ATTN: OP 981N1
ATTN: OP 223

Office of Naval Research
ATTN: Code 474, N. Perrone

Strategic Systems Project Office
ATTN: NSP-272
ATTN: NSP-43
ATTN: NSP-273

DEPARTMENT OF THE AIR FORCE

Air Force Institute of Technology
ATTN: Cmdr
ATTN: Library

Air Force Systems Cmd
ATTN: DLW

Air Force Wpns Lab
ATTN: NTES-G, S. Melzer
ATTN: NTE, M. Plamondon
ATTN: NTES-C, R. Henny
ATTN: SUL
ATTN: NTED

Assistant Chief of Staff
Intelligence
ATTN: IN

Ballistic Missile Office
ATTN: DEB

Deputy Chief of Staff
Research, Development, & Acq
ATTN: AFRDQI
ATTN: R. Steere

Deputy Chief of Staff
Logistics & Engrg
ATTN: LEEE

Foreign Technology Division
ATTN: NIIS Library
ATTN: TQTD
ATTN: SDBG
ATTN: SDBF, S. Spring

Rome Air Development Ctr
ATTN: RBES, R. Mair
ATTN: Cmdr
ATTN: TSLD

Strategic Air Command
ATTN: NRI-STINFO Library

OTHER GOVERNMENT AGENCIES

Central Intelligence Agency
ATTN: OSWR/NED
ATTN: OSR/SE/F

Department of the Interior
US Geological Survey
ATTN: D. Roddy

Federal Emergency Management Agency
ATTN: Asst Assoc Dir for Rsch, J. Kerr
ATTN: W. Chipman/NP-CP

NASA
ATTN: F. Nichols
ATTN: R. Jackson

US Nuclear Regulatory Commission
ATTN: R. Whipp for Div Sec L. Shao

NATO

NATO School (SHAPE)
ATTN: US Doc Ofcr

DEPARTMENT OF ENERGY

Department of Energy
ATTN: CTID

Department of Energy
ATTN: OMA/RD&T

Department of Energy
ATTN: Doc Con for Tech Library

DEPARTMENT OF ENERGY CONTRACTORS

University of California
Lawrence Livermore National Lab
ATTN: S. Erickson

Los Alamos National Lab
ATTN: R. Whitaker
ATTN: MS530, G. Spillman
ATTN: Reports Library
ATTN: M/S634, T. Dowler
ATTN: R. Sanford
ATTN: MS 670, J. Hopkins

Oak Ridge National Lab
ATTN: Civil Def Res Proj
ATTN: Central Rsch Library

Sandia National Lab
ATTN: Tech Lib 3141
ATTN: L. Vortman

Sandia National Labs, Livermore
ATTN: Library & Sec Class Div

DEPARTMENT OF DEFENSE CONTRACTORS

Applied Research Associates, Inc
ATTN: D. Piepenburg

Applied Research Associates, Inc
ATTN: B. Frank

BDM Corp
ATTN: T. Neighbors
ATTN: A. Lavagnino
ATTN: Corp Library

California Institute of Technology
ATTN: T. Ahrens

California Research & Technology, Inc
ATTN: M. Rosenblatt
ATTN: S. Schuster
ATTN: Library
ATTN: K. Kreyenhagen

Columbia University
ATTN: H. Bleich
ATTN: F. Dimaggio

University of Denver
ATTN: Sec Ofcr for J. Wisotski

Electric Power Research Institute
ATTN: G. Sliter

Electro-Mech Systems, Inc
ATTN: R. Shunk

DEPARTMENT OF DEFENSE CONTRACTORS (Continued)

General Dynamics Corp
ATTN: J. Miller
ATTN: J. Mador
ATTN: M. Pakstys

Kaman AviDyne
ATTN: R. Ruetenik
ATTN: G. Zartarian
ATTN: Library
ATTN: N. Hobbs

Kaman Sciences Corp
ATTN: Library
ATTN: F. Shelton

Kaman Sciences Corp
ATTN: D. Sachs

Kaman Tempo
ATTN: DASIAC

Karagozian and Case
ATTN: J. Karagozian

Lockheed Missiles & Space Co, Inc
ATTN: Tech Info Ctr
ATTN: T. Geers
ATTN: B. Almroth

Lockheed Missiles & Space Co, Inc
ATTN: TIC-Library

M&T Co
ATTN: D. McNaight

Management Science Associates
ATTN: K. Kaplan

McDonnell Douglas Corp
ATTN: R. Halprin

NKF Engrg Associates, Inc
ATTN: R. Belsheim

Pacific-Sierra Research Corp
ATTN: H. Brode, Chairman SAGE

Pacifica Technology
ATTN: R. Bjork
ATTN: G. Kent
ATTN: A. Kushner

Physics International Co
ATTN: L. Behrmann
ATTN: F. Sauer
ATTN: J. Thomsen
ATTN: E. Moore
ATTN: Tech Library

DEPARTMENT OF DEFENSE CONTRACTORS (Continued)

Physics Applications, Inc
ATTN: C. Vincent

S-CUBED
ATTN: T. Cherry
ATTN: R. Sedgewick
ATTN: D. Grine
ATTN: T. Riney
ATTN: Library
ATTN: K. Pyatt
ATTN: T. McKinley

Science Applications, Inc
ATTN: Tech Library

Southwest Research Institute
ATTN: A. Wenzel
ATTN: W. Baker

SRI International
ATTN: G. Abrahamson
ATTN: W. Wilkinson
ATTN: A. Florence

Teledyne Brown Engineering
ATTN: J. Ravenscraft

Tetra Tech, Inc
ATTN: L. Hwang

TRW Electronics & Defense Sector
ATTN: P. Bhuta
ATTN: A. Feldman
ATTN: N. Lipner
ATTN: Tech Info Ctr
ATTN: D. Jortner
ATTN: B. Sussholtz

TRW Electronics & Defense Sector
ATTN: P. Dai
ATTN: F. Pieper
ATTN: E. Wong
ATTN: G. Hulcher

Weidlinger Assoc, Consulting Engrg
ATTN: J. McCormick
ATTN: M. Baron
4 cy ATTN: R. Atkatsh
4 cy ATTN: M. Bieniek
4 cy ATTN: I. Sandler

Weidlinger Associates
ATTN: J. Isenberg

FIG. 21

53

END

FILMED

9-83

DTIC